

SUPPORTING INFORMATION FOR:

**An Fe-N<sub>2</sub> complex that generates hydrazine and ammonia via  
Fe=NNH<sub>2</sub>: Demonstrating a hybrid distal-to-alternating pathway  
for N<sub>2</sub> reduction**

Jonathan Rittle and Jonas C. Peters

Division of Chemistry and Chemical Engineering, California Institute of Technology (Caltech),

Pasadena, California 91125, United States

## Experimental Part

**General Considerations.** All manipulations were carried out using standard Schlenk or glovebox techniques under an N<sub>2</sub> atmosphere. Unless otherwise noted, solvents were deoxygenated and dried by thoroughly sparging with N<sub>2</sub> gas followed by passage through an activated alumina column in the solvent purification system by SG Water, USA LLC. Non-halogenated solvents were tested with a standard purple solution of sodium benzophenone ketyl in tetrahydrofuran in order to confirm effective oxygen and moisture removal. All reagents were purchased from commercial vendors and used without further purification unless otherwise stated. {K(Et<sub>2</sub>O)} {[SiP<sup>iPr</sup><sub>3</sub>]Fe-N<sub>2</sub>} (**1**),<sup>1</sup> {[SiP<sup>iPr</sup><sub>3</sub>]Fe-NH<sub>2</sub>NH<sub>2</sub>} {BAR<sup>F</sup><sub>24</sub>}<sup>1</sup>, {[SiP<sup>iPr</sup><sub>3</sub>]Fe-NH<sub>2</sub>NH<sub>2</sub>} {OTf},<sup>1</sup> {H(OEt<sub>2</sub>)<sub>2</sub>} {BAR<sup>F</sup><sub>24</sub>}<sup>2</sup> and anhydrous <sup>57</sup>FeCl<sub>2</sub><sup>3</sup> were synthesized following literature procedures with slight modifications. <sup>57</sup>Fe-enriched **1** was obtained via [SiP<sup>iPr</sup><sub>3</sub>]<sup>57</sup>Fe(Cl) by replacing FeCl<sub>2</sub> with <sup>57</sup>FeCl<sub>2</sub>.<sup>1</sup> Deuterated solvents were purchased from Cambridge Isotope Laboratories, Inc., degassed and stored over activated 3 Å molecular sieves prior to use. Elemental analyses were performed by Midwest Microlab, LLC, Indianapolis, IN. <sup>1</sup>H, <sup>13</sup>C and <sup>29</sup>Si chemical shifts are reported in ppm relative to tetramethylsilane, using residual solvent resonances as internal standards. <sup>31</sup>P chemical shifts are reported in ppm relative to 85% aqueous H<sub>3</sub>PO<sub>4</sub>. <sup>15</sup>N chemical shifts are reported in ppm relative to liquid NH<sub>3</sub> at 0 ppm and internally referenced to CD<sub>3</sub>C<sup>15</sup>N at 242.6 ppm. Solution phase magnetic measurements were performed by the method of Evans.<sup>4</sup> Solid IR measurements were obtained on a Bruker Alpha spectrometer equipped with a diamond ATR probe.

**EPR Spectroscopy.** X-band EPR spectra were obtained on a Bruker EMX spectrometer on 2-5 mM solutions prepared as frozen glasses in 2-MeTHF. Samples were collected at powers ranging from 20 μW to 15 mW and modulation amplitudes of 1 – 5 Gauss. Spectra were simulated using the EasySpin<sup>5</sup> suite of programs with Matlab 2013.

**Optical Spectroscopy.** Measurements were taken on a Cary 50 UV-Visible spectrophotometer using a 1-cm quartz cell connected to a round-bottom flask and sealed with a Teflon stopcock. Variable temperature measurements were collected with a Unisoku CoolSpek cryostat mounted within the Cary spectrophotometer. Spectra of **5'** were obtained by charging the cuvette with solid **5'** and a flea stir bar, followed by evacuation of the headspace and sealing the Teflon stopcock. The adjacent compartment was charged with THF and sealed after application of mild vacuum. The cuvette was then mounted within the Unisoku cryostat and chilled to the desired temperature. Stirring was commenced and the stopcock separating the two compartments was opened and allowing the THF to transfer *in vacuo* and dissolve **5'** at the desired temperature.

**X-Ray Crystallography.** XRD studies were carried out at the Beckman Institute Crystallography Facility on a Bruker Kappa Apex II diffractometer (Mo Kα radiation). Structures were solved using SHELXS or SHELXT and refined against F<sup>2</sup> on all data by full-matrix least squares with SHELXL. The crystals were mounted on a glass fiber under Paratone N oil. See below for any special refinement details for individual data sets.

**Electrochemistry.** Electrochemical measurements were carried out in a thick-walled one-component electrochemical cell fitted with a Teflon stopcock and tungsten leads protruding from the top of apparatus. A CD instruments 600B electrochemical analyzer was used for data collection. A freshly-polished glassy carbon electrode was used as the working electrode and platinum wire was used as the auxiliary electrode. Solutions (THF) of electrolyte (0.1 M tetra-*n*-butylammonium hexafluorophosphate) contained ferrocene (1 mM), to serve as an internal

reference, and analyte (1 mM). All reported potentials are referenced to the ferrocene couple,  $\text{Cp}_2\text{Fe}^+/\text{Cp}_2\text{Fe}$ .

**$^{57}\text{Fe}$  Mössbauer Spectroscopy.** Spectra were recorded on a spectrometer from SEE Co (Edina, MN) operating in the constant acceleration mode in a transmission geometry. The sample was kept in an SVT-400 cryostat from Janis (Wilmington, MA). The quoted isomer shifts are relative to the centroid of the spectrum of a metallic foil of  $\alpha\text{-Fe}$  at room temperature. Solid samples were prepared by grinding polycrystalline material into a fine powder and then mounted in a Delrin cup fitted with a screw-cap as a boron nitride pellet. Solution samples were transferred to a sample cup chilled to 77K inside of the glovebox. Upon freezing of the solution, the cup was quickly removed from the glovebox and immersed in liquid  $\text{N}_2$  until being mounted in the cryostat. Data analysis was performed using the program WMOSS ([www.wmoss.org](http://www.wmoss.org)) and quadrupole doublets were fit to Lorentzian lineshapes.

Features undergoing slow electronic relaxation in the magnetically-perturbed Mossbauer data were fit in the  $S = 1/2$  representation. The Hamiltonian in this representation is given by,

$$\mathcal{H} = \beta \vec{S} \cdot \mathbf{g} \cdot \vec{B} + \vec{S} \cdot \mathbf{A} \cdot \vec{I} + \mathcal{H}_Q \quad \text{Eqn S1}$$

$$\mathcal{H}_Q = \left( \frac{eQV_{zz}}{12} \right) \left[ 3I_z^2 - \frac{15}{4} + \eta(I_x^2 - I_y^2) \right] \quad \text{Eqn S2}$$

Where  $\mathbf{g}$  is the  $\mathbf{g}$  tensor obtained by EPR simulation,  $\mathbf{A}$  is the  $^{57}\text{Fe}$  hyperfine tensor,  $\mathcal{H}_Q$  is the nuclear quadrupole interaction of the  $I = 3/2$  excited state, and  $\eta = (V_{xx} - V_{yy}) / V_{zz}$  is the asymmetry parameter.<sup>6</sup>

**DFT Calculations.** Geometry optimizations, single-point calculations and frequency calculations were performed using the Gaussian 09 (Rev B.01) suite of programs with the BP86 functional, the 6-31G(d) basis set for C and H atoms, and the def2TZVPP basis set for Fe, P, Si and N atoms.<sup>7</sup> Frequency calculations were performed on optimized geometries to ensure true minima. Initial guesses for geometry optimizations were obtained, when possible, from coordinates derived from X-ray crystallography. For the optimized structure of compound **7**, the XRD coordinates of **8** were used as an initial guess with the  $(\text{NNMe}_2)$  fragment truncated to  $(\text{NNH}_2)$ . Free energies were computed from frequency calculations.

### Synthetic Procedures

**$\{\{\text{SiP}^{\text{iPr}}_3\}\text{Fe}=\text{NNH}_2\}\{\text{OTf}\}$  (**5'**).** In the glovebox, complex **1** (0.125 g, 150  $\mu\text{mol}$ ) was dissolved in 2-MeTHF (4 mL) and this solution was filtered into a 20-mL scintillation vial that was subsequently frozen in a coldwell chilled externally with liquid nitrogen. A second scintillation vial was charged with HOTf (0.068 g, 453  $\mu\text{mol}$ ) and 2-MeTHF (4 mL) and similarly frozen in the cold well. The acid solution was briefly thawed and layered on top of the frozen Fe-containing solution followed by refreezing the solutions. To combine the two layers, the vial was elevated off of the floor of the coldwell with forceps, and a pre-chilled spatula was used to mechanically stir the two layers until homogenous. (NOTE: It is critical to combine the layers as soon as the solvent glass melts and while the solution remains rather viscous.) The resulting solution was layered with pre-chilled pentane (15 mL) and the layers were mixed with the spatula, causing the formation of a purple precipitate. This solid was separated via gravity filtration through a medium frit at  $-78^\circ\text{C}$  and subsequently washed with additional, chilled pentane (2 x 20 mL), toluene (2 x 10 mL) then pentane (2 x 5 mL). 63.7 mg of **5'** was obtained as a purple solid (<49 % yield) after drying *in vacuo*. **5'** prepared in this manner was found to be

free of Fe-containing impurities, as judged by  $^{57}\text{Fe}$  Mössbauer spectroscopy, but contains variable amounts of KOTf that is evident in the solid IR spectra. Attempts to free **5'** from this salt have been unsuccessful. Single crystals of **5'** suitable for X-ray diffraction were obtained by layering a concentrated 2-MeTHF solution of **5'** with pentane at  $-78^\circ\text{C}$  and allowing the mixture to stand for 16 hours.  $^1\text{H}$  NMR (500 MHz, 9:1 THF- $d_8$ :  $\text{CD}_3\text{CN}$ , 233 K, ppm): 9.50 (bs, 2H,  $\text{NNH}_2$ ).  $^{31}\text{P}\{^1\text{H}\}$  NMR (202.4 MHz, 9:1 THF- $d_8$ :  $\text{CD}_3\text{CN}$ , 193 K, ppm): 95.5 (bs).  $^{29}\text{Si}\{^1\text{H}\}$  NMR (99.3 MHz, 9:1 THF- $d_8$ :  $\text{CD}_3\text{CN}$ , 193 K, ppm): 81.4 (m, FWHM = 100 Hz). UV-Visible (THF, 193 K,  $\text{nm}\{\text{cm}^{-1}\text{M}^{-1}\}$ ): 528 {1480}, 742 {536}. IR (Solid, 298 K,  $\text{cm}^{-1}$ ): 3207, 3039, 1627, 1443, 826.

$\{\{\text{SiP}^{\text{iPr}}_3\}\text{Fe}=\text{}^{15}\text{N}^{15}\text{NH}_2\}\{\text{OTf}\}$  ( $^{15}\text{N}$ -**5'**). Prepared in an analogous fashion to **5'** but employing  $^{15}\text{N}$ -**1**.  $^1\text{H}$  NMR (500 MHz, 9:1 THF- $d_8$ :  $\text{CD}_3\text{CN}$ , 233 K, ppm): 9.50 (d,  $^1\text{J}_{\text{NH}}$ : 97 Hz, 2H,  $\text{NNH}_2$ ).  $^{15}\text{N}$  NMR (50.6 MHz, 9:1 THF- $d_8$ :  $\text{CD}_3\text{CN}$ , 213 K, ppm): 517.54 (bs, FWHM = 36 Hz), 198.45 (td,  $^1\text{J}_{\text{NH}}$ : 96 Hz,  $^1\text{J}_{\text{NN}}$ : 11 Hz). IR (Solid, 298 K,  $\text{cm}^{-1}$ ): 1623, 1401, 803.

$\{\{\text{SiP}^{\text{iPr}}_3\}\text{Fe}=\text{NND}_2\}\{\text{OTf}\}$  (**5'**- $d_2$ ). Prepared in an analogous fashion to **5'** but employing HOTf- $d_1$ . IR (Solid,  $\text{cm}^{-1}$ ): 2380, 2241.

$\{\{\text{SiP}^{\text{iPr}}_3\}\text{Fe}=\text{NNMe}_2\}\{\text{OTf}\}$  (**6**). In the glovebox, complex **1** (0.235 g, 293  $\mu\text{mol}$ ), a magnetic stir bar, and 1,2-dimethoxyethane (6 mL) were charged into a 20 mL scintillation vial and chilled to  $-78^\circ\text{C}$  in the coldwell. Stirring was commenced and methyl trifluoromethanesulfonate (100  $\mu\text{L}$ , 911  $\mu\text{mol}$ ) was added in one portion via syringe. The solution was allowed to stir at this temperature for 90 minutes, resulting in a dark-amber solution. The vial was subsequently evacuated and slowly warmed to 298 K while solvent was removed *in vacuo*. Purple solids deposit during this process. The solids were transferred to a medium frit and washed at room temperature with benzene (3 x 10 mL), 1,2-dimethoxyethane (3 x 5 mL), and  $\text{Et}_2\text{O}$  (5 mL), followed by extraction into  $\text{CH}_3\text{CN}$  (10 mL) and concentration *in vacuo*. The resulting film was triturated with  $\text{Et}_2\text{O}$  and dried *in vacuo* to afford 116 mg of **6** (45 % yield) as an analytically-pure, free-flowing purple powder. Single crystals suitable for X-ray diffraction were obtained by slow diffusion of  $\text{Et}_2\text{O}$  into a concentrated  $\text{CH}_3\text{CN}$  solution of **6** at 298 K.  $^1\text{H}$  NMR (500 MHz,  $\text{CD}_3\text{CN}$ , 293 K, ppm): 8.08 (3H, d, 7.3 Hz), 7.70 (3H, d, 7.6 Hz), 7.50 (3H, t, 7.3 Hz), 7.39 (3H, t, 7.6 Hz), 2.95 (6H, s), 2.46 (6H, hept, 6.7 Hz), 1.21 (18H, bs), 0.67 (18H, bs).  $^{13}\text{C}$  NMR (125.7 MHz,  $\text{CD}_3\text{CN}$ , 293 K, ppm): 156.18, 143.19, 132.22, 130.78, 130.54, 128.58, 53.93, 31.79, 19.94.  $^{29}\text{Si}\{^1\text{H}\}$  NMR (99.3 MHz,  $\text{CD}_3\text{CN}$ , 233 K, ppm): 74.2 (bq,  $^2\text{J}_{\text{SiP}}$  = 33 Hz).  $^{31}\text{P}\{^1\text{H}\}$  NMR (202.4 MHz,  $\text{CD}_3\text{CN}$ , 233 K, ppm): 94.9 (bs). UV-Visible (THF, 298K,  $\text{nm}\{\text{cm}^{-1}\text{M}^{-1}\}$ ): 543 {1340}, 745 {430}. IR (Solid,  $\text{cm}^{-1}$ ): 1498, 1373, 858. Anal: calc. for  $\text{C}_{39}\text{H}_{60}\text{F}_3\text{FeN}_2\text{O}_3\text{P}_3\text{SSi}$ : C 53.79, H 6.95, N 3.22; found: C 53.96, H 6.84, N 3.27.

$\{\{\text{SiP}^{\text{iPr}}_3\}\text{Fe}=\text{}^{15}\text{N}^{15}\text{NMe}_2\}\{\text{OTf}\}$  ( $^{15}\text{N}$ -**6**). Prepared in an analogous fashion to **6** but employing  $^{15}\text{N}$ -**1**.  $^{15}\text{N}$  NMR (50.6 MHz,  $\text{CD}_3\text{CN}$ , 298 K, ppm): 530.4 (m, FWHM= 24 Hz), 184.7 (d,  $^1\text{J}_{\text{NN}}$ : 11.5 Hz). IR (Solid,  $\text{cm}^{-1}$ ): 1474, 1354, 847.

$\{\{\text{SiP}^{\text{iPr}}_3\}\text{Fe}=\text{NN}(\text{CD}_3)_2\}\{\text{OTf}\}$  (**6**- $d_6$ ). Prepared in an analogous fashion to **6** but employing MeOTf- $d_3$ . IR (Solid,  $\text{cm}^{-1}$ ): 1439.

$\{\{\text{SiP}^{\text{iPr}}_3\}\text{Fe}=\text{}^{15}\text{N}^{15}\text{N}(\text{CD}_3)_2\}\{\text{OTf}\}$  ( $^{15}\text{N}$ -**6**- $d_6$ ). Prepared in an analogous fashion to **6** but employing MeOTf- $d_3$  and  $^{15}\text{N}$ -**1**. IR (Solid,  $\text{cm}^{-1}$ ): 1399.

$[\text{SiP}^{\text{iPr}}_3]\text{Fe}=\text{NNH}_2$  (**7**). *Preparation of EPR samples.* In the glovebox, a quartz EPR tube pre-chilled in a cold well by an external liquid nitrogen bath was charged with a thawing 5 mM solution of **5'** in 2-MeTHF (150  $\mu\text{L}$ ). This solution was frozen and a thawing 5 mM solution of

Cp\*<sub>2</sub>Co in 2-MeTHF (150 μL) was layered on top of the frozen solution of **5'**. A pre-chilled steel cannula was inserted into the EPR tube. The tube was elevated off of the floor of the cold well, partially melting the solutions. While still viscous, the solutions were agitated with the cannula for 3 minutes or until the mixture appeared homogeneous. The cannula was removed and the solution was refrozen in the cold well. EPR tubes were quickly removed from the glovebox and stored in liquid nitrogen prior to the collection of EPR data.

[SiP<sup>iPr</sup><sub>3</sub>]Fe=NND<sub>2</sub> (**7-d<sub>2</sub>**). EPR samples were obtained in an identical fashion to **7** but employ **5'-d<sub>2</sub>** as a reagent.

[SiP<sup>iPr</sup><sub>3</sub>]<sup>57</sup>Fe=NNH<sub>2</sub> (**<sup>57</sup>Fe-7**). *Preparation of <sup>57</sup>Fe Mössbauer samples.* In the glovebox, a 1 mL Delrin cup, pre-chilled to 77K in a cold well by an external liquid nitrogen bath, was charged with a thawing 5 mM solution of <sup>57</sup>Fe-**5'** in 2-MeTHF (300 μL). This solution was frozen and a thawing 5 mM solution of Cp\*<sub>2</sub>Co in 2-MeTHF (300 μL) was layered on top of the frozen solution of <sup>57</sup>Fe-**5'** and similarly frozen. A pre-chilled steel spatula was inserted into the cup. Using pre-chilled forceps, the cup was elevated off of the floor of the cold well, partially melting the solutions. While still viscous, the solutions were gently agitated with the spatula for 10 minutes or until the mixture appeared homogeneous. The solutions were periodically refrozen by lowering the cup back on to the cold well floor to prevent thermal decomposition of <sup>57</sup>Fe-**7**. The spatula was finally removed and the solution was refrozen in the cold well. The cup was quickly removed from the glovebox and stored in liquid nitrogen prior to the collection of Mössbauer data.

[SiP<sup>iPr</sup><sub>3</sub>]Fe=NNMe<sub>2</sub> (**8**). In the glovebox, **6** (45 mg, 51.7 μmol) was suspended in 2-MeTHF (2 mL) and stirred at rt. A portion of 0.5 % Na(Hg) (2.0 mg Na, 87.0 μmol) was added, causing an immediate darkening of the solution. The reaction mixture was concentrated to dryness *in vacuo* after 5 minutes of stirring and the dark brown residue was extracted with pentane (2 x 5 mL). The solution was concentrated to dryness *in vacuo* affording 18 mg of **6** (48% yield). Complex **6** decays to a mixture of **2** and [SiP<sup>iPr</sup><sub>3</sub>]Fe(H)N<sub>2</sub> overnight at room temperature as judged by <sup>1</sup>H NMR spectroscopy. Therefore, combustion analysis was not obtained. Single crystals suitable for X-ray diffraction were obtained by storing a saturated pentane solution of **8** at -35 °C overnight. <sup>1</sup>H NMR (500 MHz, C<sub>6</sub>D<sub>6</sub>, 298 K, ppm): 7.69, 6.36, 4.76. UV-Visible (THF, 298K, nm {cm<sup>-1</sup> M<sup>-1</sup>}): 320 {7700}, 428 {3380}, 536 (sh) {2040}, 985 {170}. IR (Solid, cm<sup>-1</sup>): 1331, 1125, 838. μ<sub>eff</sub> (C<sub>6</sub>D<sub>6</sub>, 298 K): 1.7μ<sub>B</sub>.

**Formation of **9** and **2** from Isolated **5'**.** In the glovebox, complex **5'** (10.0 mg, 12 μmol) and a magnetic stir bar were charged into a 20 mL scintillation vial and cooled to -78 °C in the coldwell. Similarly-chilled THF (2 mL) was added and the mixture was stirred for 20 minutes or until all of the solids had dissolved. The solution was subsequently frozen at liquid nitrogen temperatures, and a solution of Cp\*<sub>2</sub>Co (3.8 mg, 11 μmol) in THF (2 mL) was layered on top and similarly frozen. The external liquid nitrogen bath was subsequently removed, and the mixture was allowed to slowly warm to room temperature with vigorous stirring over 10 minutes. At this point, the solution was filtered and concentrated to dryness *in vacuo*. The remaining orange residue was dissolved in C<sub>6</sub>D<sub>6</sub> (500 μL), filtered and analyzed by <sup>1</sup>H NMR spectroscopy.

**One-Pot Conversion of Compound **1** to **9** and N<sub>2</sub>H<sub>4</sub> / NH<sub>3</sub> Quantitation.** In a typical run, compound **1** (19.5 mg, 24.3 μmol) was dissolved in 2-MeTHF (2 mL) and chilled to 77 K in a coldwell chilled externally with liquid nitrogen. HOTf (8 mg, 53.3 μmol) dissolved in pre-chilled 2-MeTHF (1 mL) was layered on top of this solution and subsequently frozen. The vial was elevated off of the floor of the coldwell and mechanically stirred with a pre-chilled spatula for 2 minutes, resulting in a homogenous, red-purple solution characteristic of **5'**. The solution was subsequently refrozen, and a pre-chilled solution of Cp\*<sub>2</sub>Co (4 mg, 12.1 μmol) in 2-MeTHF (2

mL) was layered on top and subsequently frozen. The vial was elevated off of the floor of the coldwell and mechanically stirred with a pre-chilled spatula for 2 minutes, resulting in a dark-brown solution color. The mixture was refrozen and a stir bar was added to the reaction vessel. The external liquid nitrogen bath was removed, allowing the mixture to slowly warm to room temperature over 10 minutes as the solution was vigorously stirred. The procedure diverges here depending on the desired analysis and is detailed below.

**For NMR analysis:**

At this point, the solution was filtered through a pad of glass filter paper and concentrated to dryness *in vacuo*. The remaining orange residue was dissolved in C<sub>6</sub>D<sub>6</sub> (500  $\mu$ L) and analyzed by <sup>1</sup>H NMR spectroscopy.

**For N<sub>2</sub>H<sub>4</sub>/NH<sub>3</sub> Quantitation:**

At this point, (or after 24 hours of continued stirring at room temperature) the reaction was quenched with HCl (1 mL, 1 M in Et<sub>2</sub>O) and stirred for 5 minutes at room temperature. Volatiles were concentrated *in vacuo* and H<sub>2</sub>O (1 mL) was added to the resulting solid residue. The resulting mixture was thoroughly agitated and sonicated for 10 minutes, and insoluble material was subsequently removed by filtration through a glass filter pad. The resulting aqueous solution was assayed for N<sub>2</sub>H<sub>4</sub> and NH<sub>3</sub> using established procedures.<sup>8,9</sup>

**NMR Spectra**

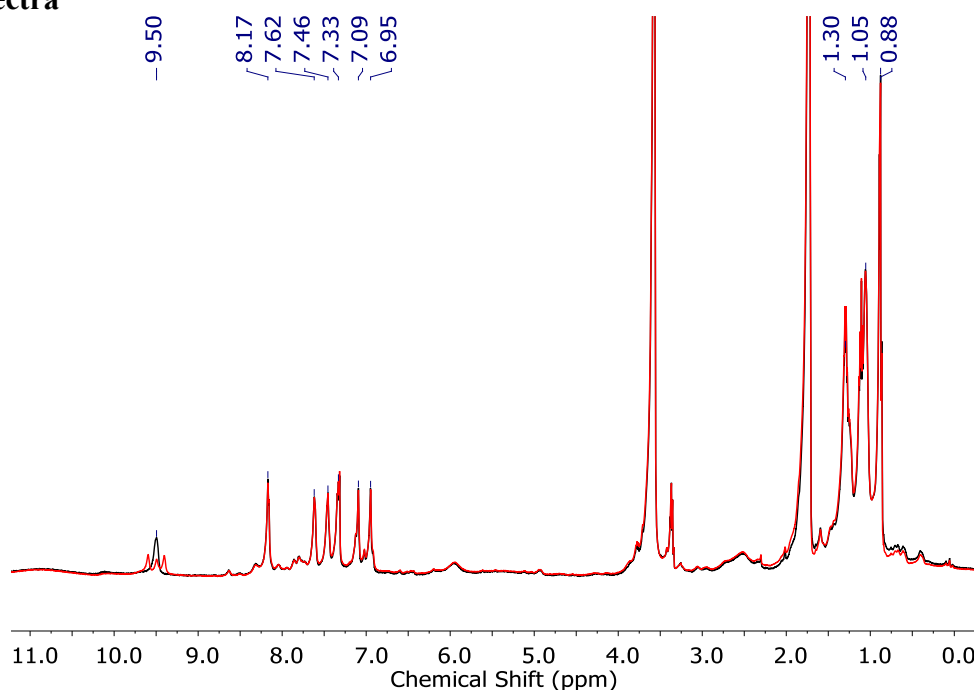


**Figure S1.** Overlaid <sup>1</sup>H NMR spectrum (500 MHz, 233K, Red) and {<sup>15</sup>N}<sup>1</sup>H NMR spectrum (Black) of <sup>15</sup>N-5' recorded in THF-*d*<sub>8</sub>. The <sup>15</sup>N decoupler window was centered at a chemical shift of 200 ppm. The broad, paramagnetically-shifted peaks scattered throughout the spectrum belong to one or more unidentified impurities that result from the partial warming of <sup>15</sup>N-5' during the sample transfer into the NMR probe.

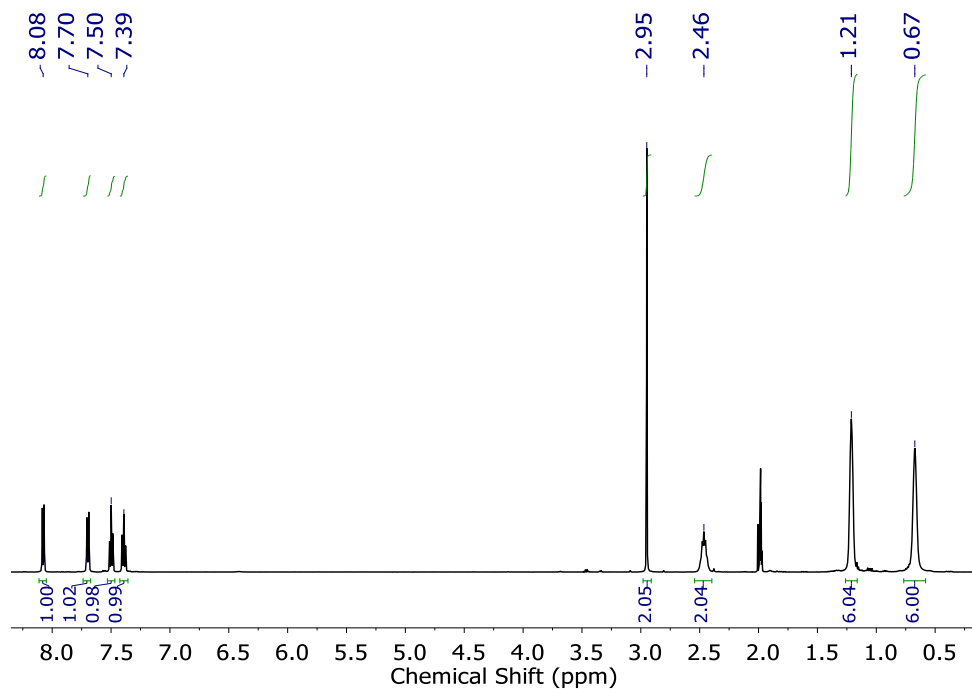


**Figure S2.**  $^1\text{H}$  NMR spectrum (500 MHz, 293K) of **6** recorded in  $\text{CD}_3\text{CN}$ .

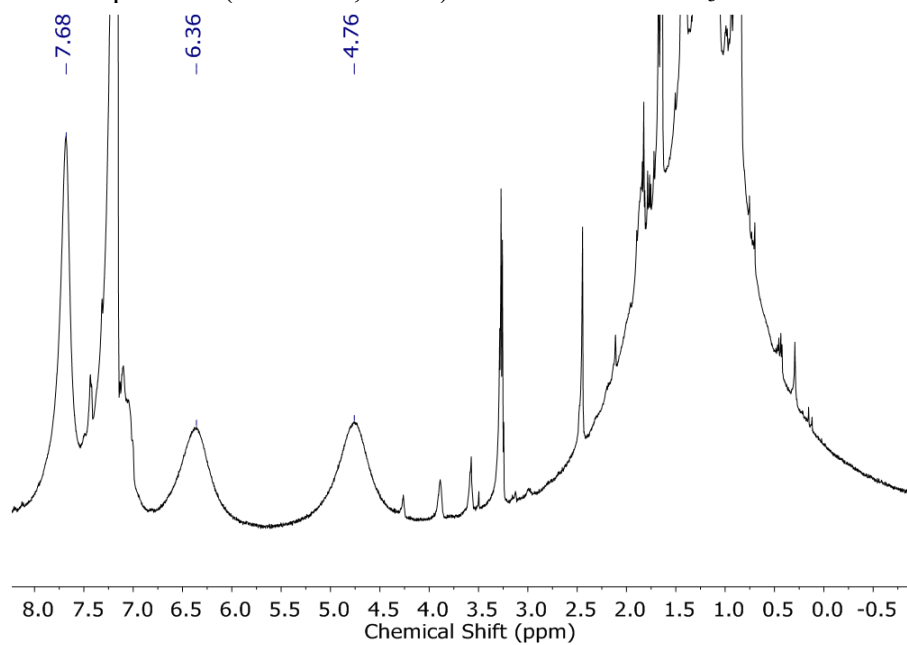


**Figure S3.**  $^1\text{H}$  NMR spectrum (500 MHz, 298K) of **8** recorded in  $\text{C}_6\text{D}_6$ .

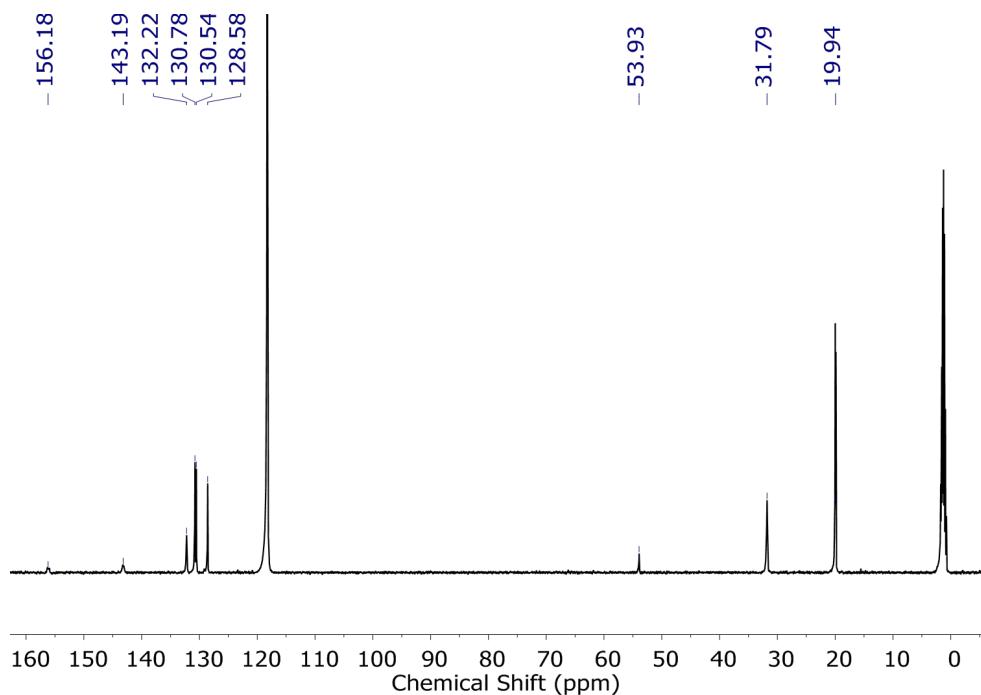


**Figure S4.**  $^{13}\text{C}$  NMR spectrum (125.7 MHz, 293 K) of **6** recorded in  $\text{CD}_3\text{CN}$ .

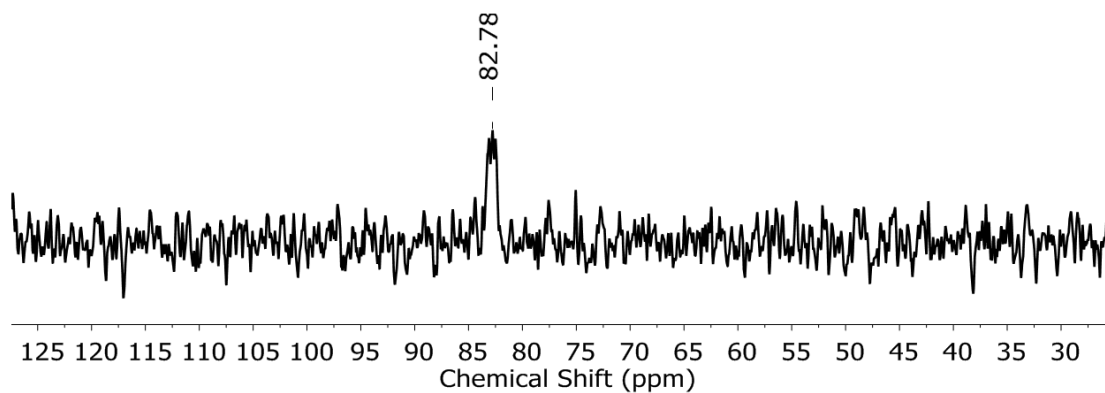


**Figure S5.**  $^{29}\text{Si}$  NMR spectrum (99.3 MHz, 193 K) of **5'** recorded in 9:1  $\text{THF}:\text{CD}_3\text{CN}$ .

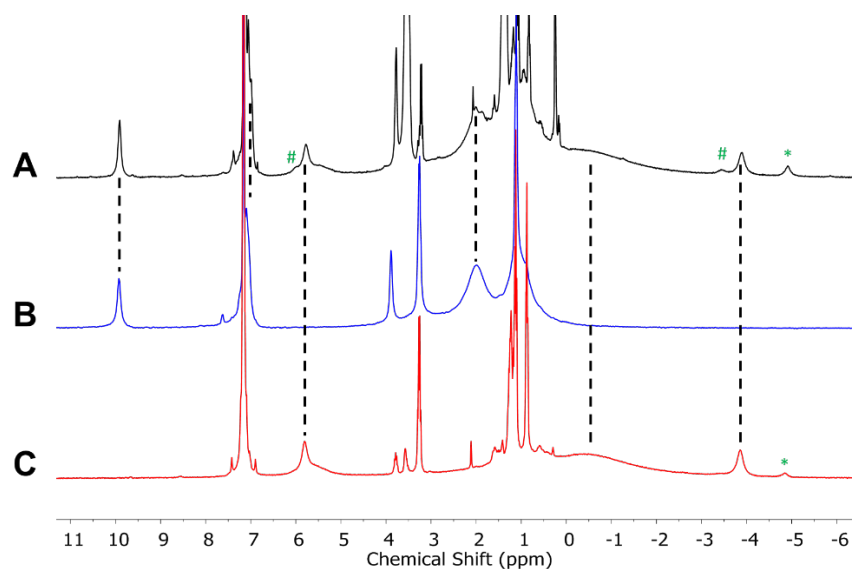


**Figure S6.** <sup>1</sup>H NMR spectra (300 MHz, 293 K, C<sub>6</sub>D<sub>6</sub>) of (A) the crude reaction mixture obtained by the reaction of **5'** with Cp\*<sub>2</sub>Co in THF followed by warming to r.t. Trace (B) corresponds to the spectrum of independently-prepared Fe-N<sub>2</sub> **2** collected under identical conditions. Trace (C) corresponds to the spectrum of independently-prepared Fe-NH<sub>2</sub>NH<sub>2</sub><sup>+</sup> **9** collected under identical conditions. Features marked with a “#” arise from Fe-NH<sub>3</sub><sup>+</sup> **11** and features marked with “\*” arise from Fe-OTf **10**. Compound **9** and **11** slowly decompose to Fe-OTf **10** in C<sub>6</sub>D<sub>6</sub> at room temperature.<sup>1</sup>

### Infrared Spectra

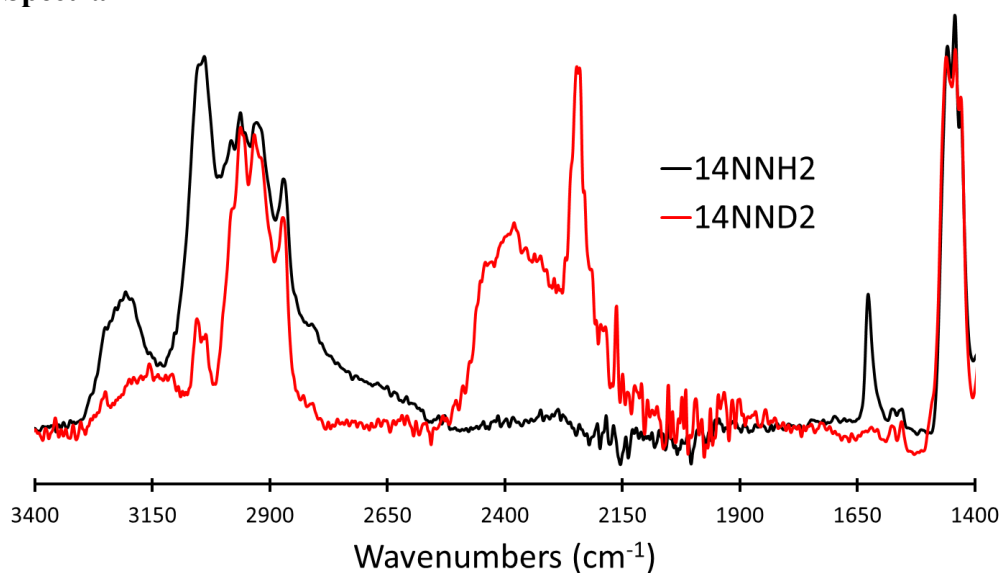


**Figure S7.** Overlaid IR absorption spectra of solid **5'** (Black), and **5'-d<sub>2</sub>** (Red).

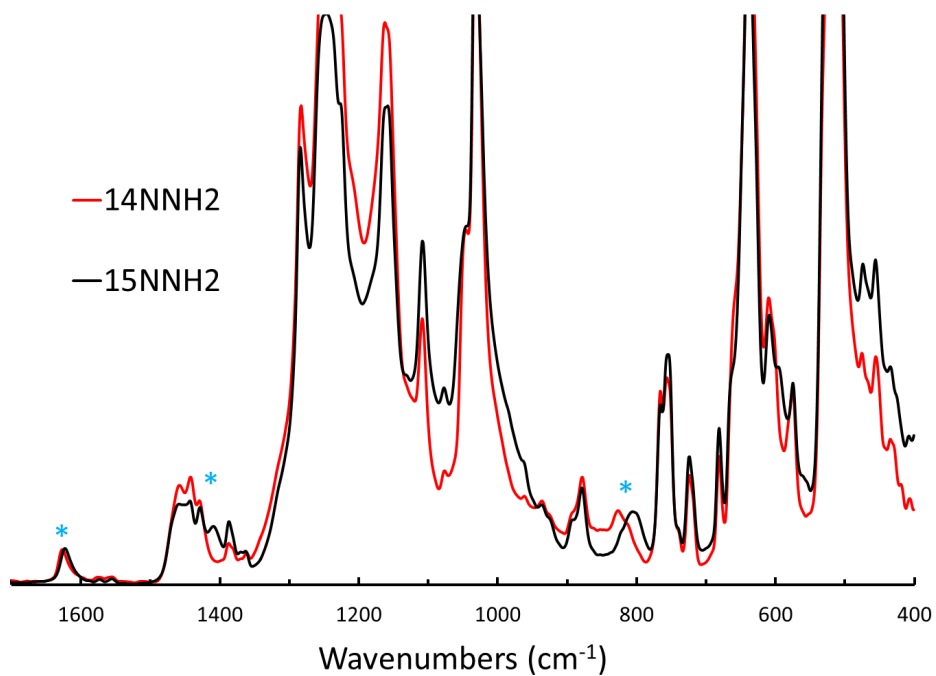


**Figure S8.** Overlaid IR absorption spectra of solid **5'** (Red), and <sup>15</sup>N-**5'** (Black).

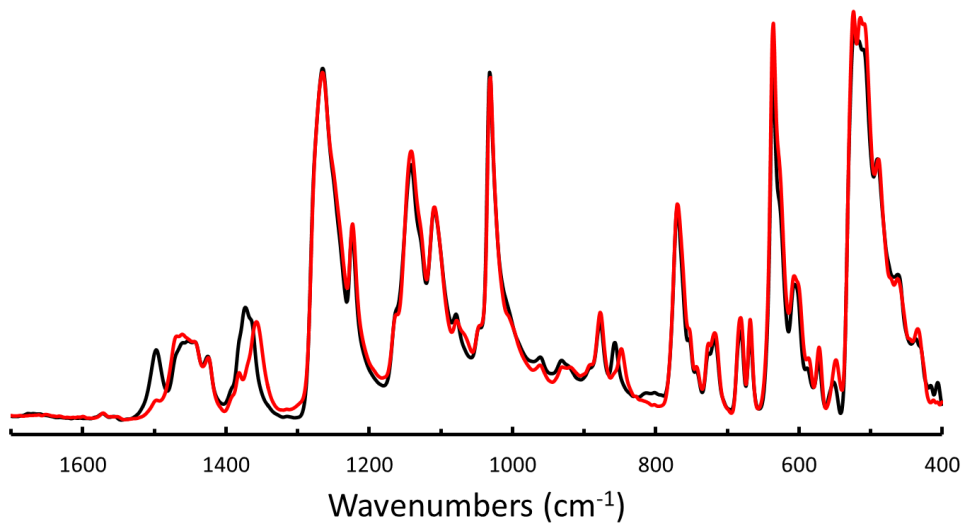


**Figure S9.** Overlaid IR absorption spectra of solid **6** (Black), and <sup>15</sup>N-**6** (Red).

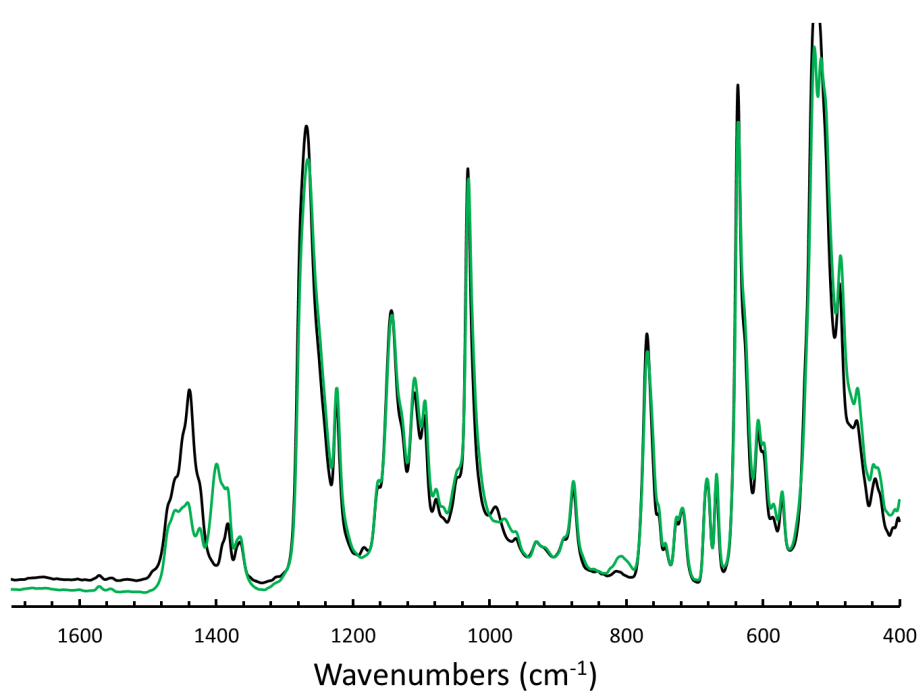


**Figure S10.** Overlaid IR absorption spectra of solid **6-d<sub>6</sub>** (Black) and **<sup>15</sup>N-6-d<sub>6</sub>** (Green).

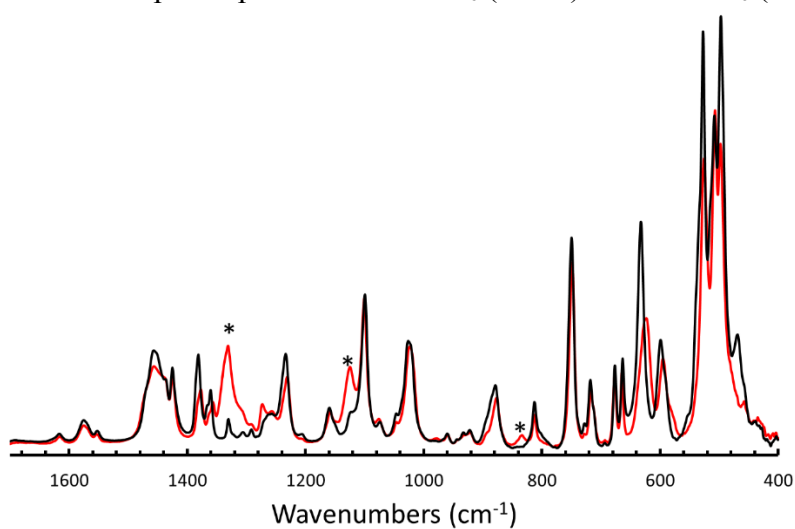


**Figure S11.** Overlaid IR absorption spectra of freshly-isolated **8** (Red) and following thermolysis at 60 °C in C<sub>6</sub>D<sub>6</sub> for 1 hour (black).

## UV-Visible Spectra

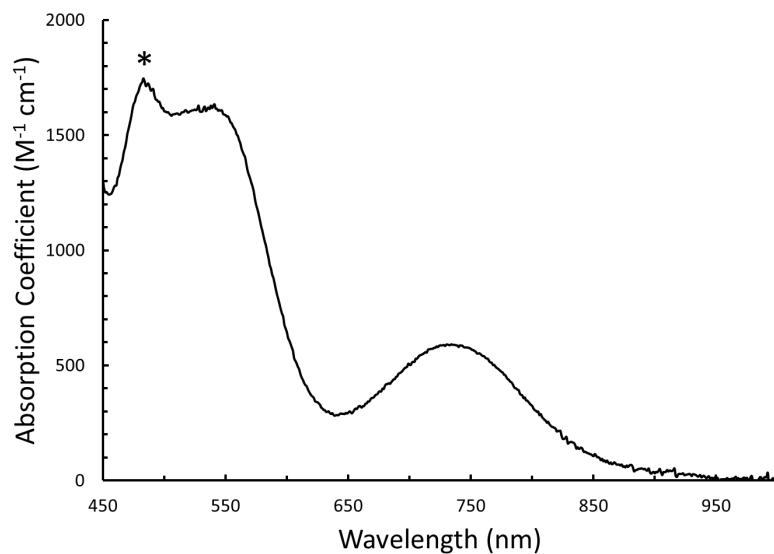


**Figure S12.** UV/visible spectra of **5'** in THF at 193 K. The asterisk denotes an absorbance derived from a small impurity ( $\sim 4\%$ ) of  $[\text{SiP}^{\text{iPr}}_3]\text{Fe-OTf}$  generated upon dissolution of **5'**. The density increase of THF at cryogenic temperatures was not accounted for.

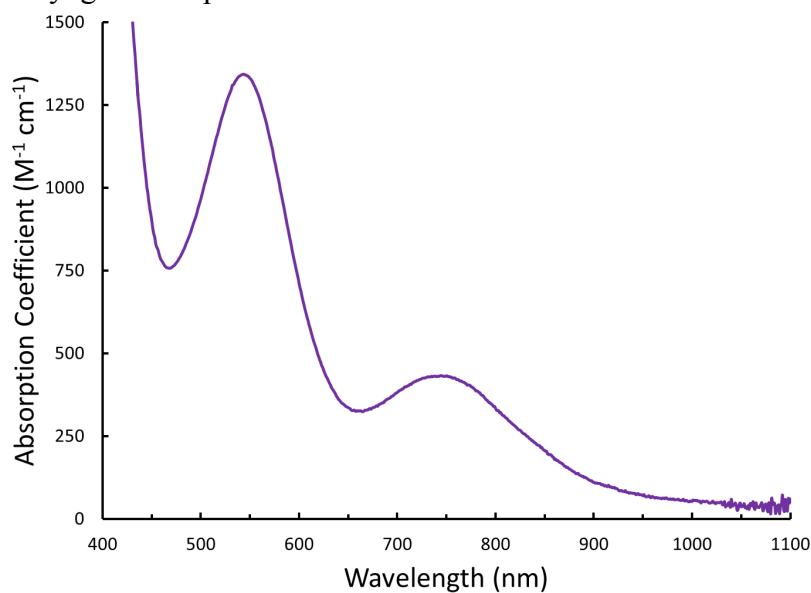


**Figure S13.** UV/visible spectra of **6** in THF at 298 K.

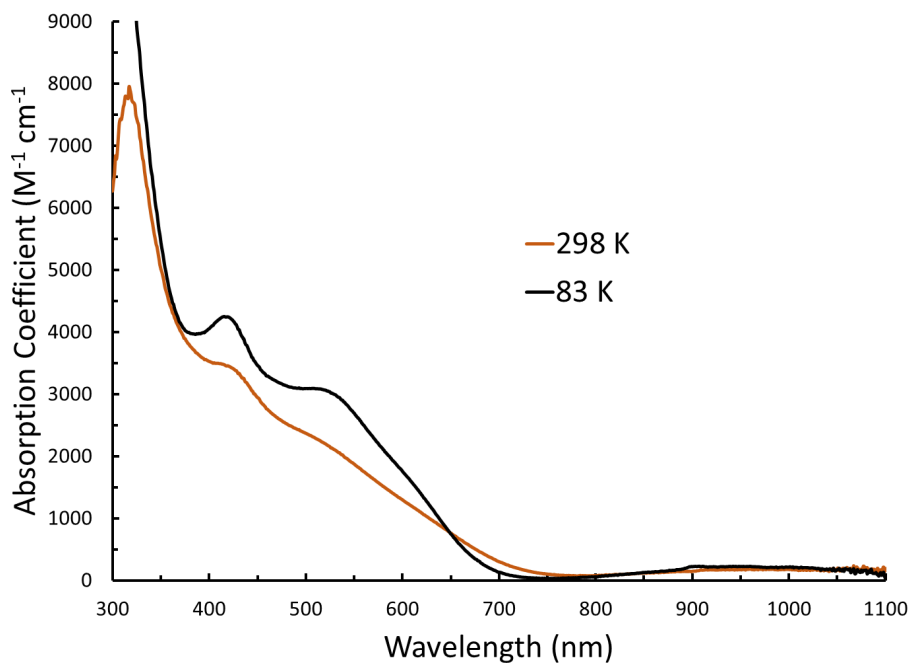


**Figure S14.** UV/visible spectra of **8** in 2-MeTHF at 298 and 83 K.

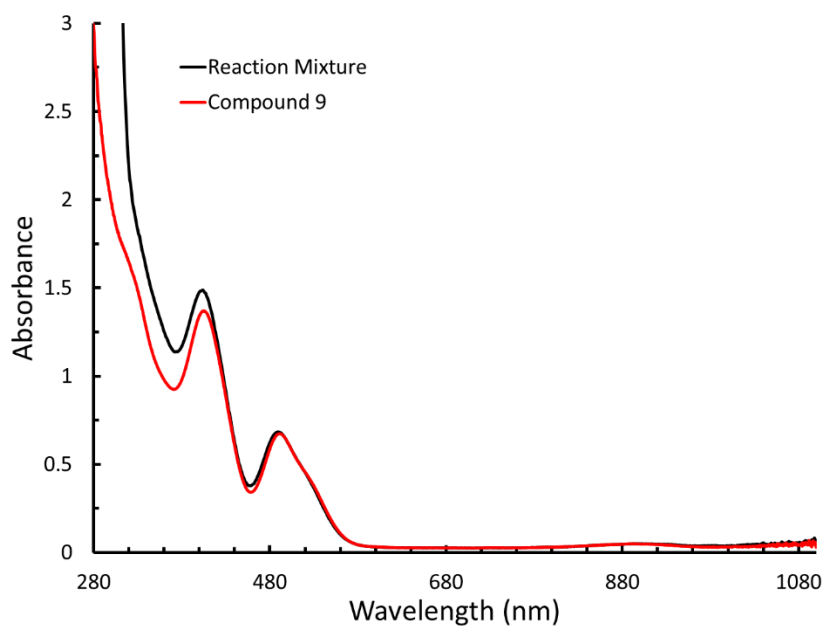


**Figure S15.** Overlaid UV-visible spectra of **9** (Red) and the solid material obtained by the reaction of **5'** with  $\text{Cp}^*_2\text{Co}$  in THF followed by warming to r.t and evaporation of solvent *in vacuo*. Compound **2** was subsequently removed from this mixture by extensive washes with pentane and the resulting orange solid was dissolved in THF and the resulting spectra is shown in Black.

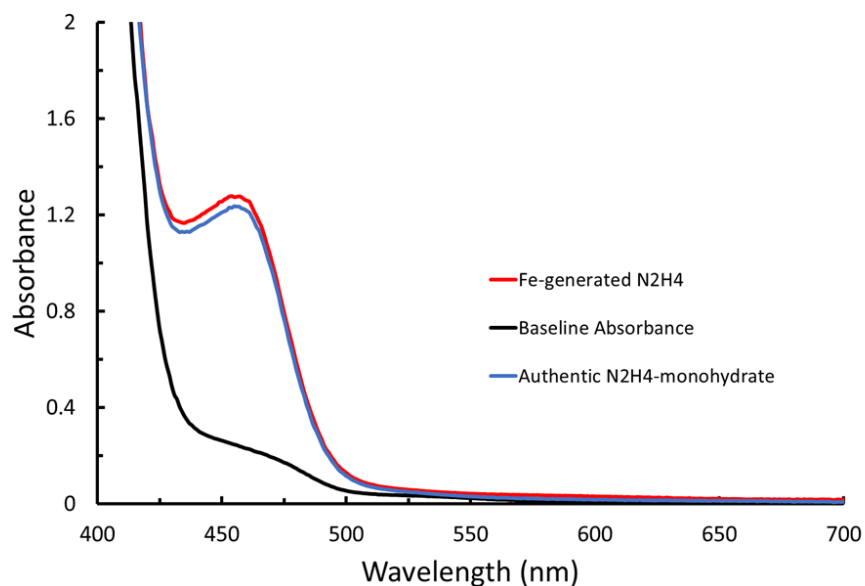


**Figure S16.** Raw UV-visible spectra obtained in the *p*-dimethylaminobenzaldehyde assay for  $\text{N}_2\text{H}_4$ . (Black) Background absorbance obtained in the absence of  $\text{N}_2\text{H}_4$ . (Red) Assay of a representative reaction mixture derived from the conversion of **5'** to **9** followed by quenching of the reaction mixture with HCl after 10 minutes. (Blue) Assay performed on a comparable amount of commercial  $\text{N}_2\text{H}_4\text{-H}_2\text{O}$ .

### $^{57}\text{Fe}$ Mössbauer Spectra

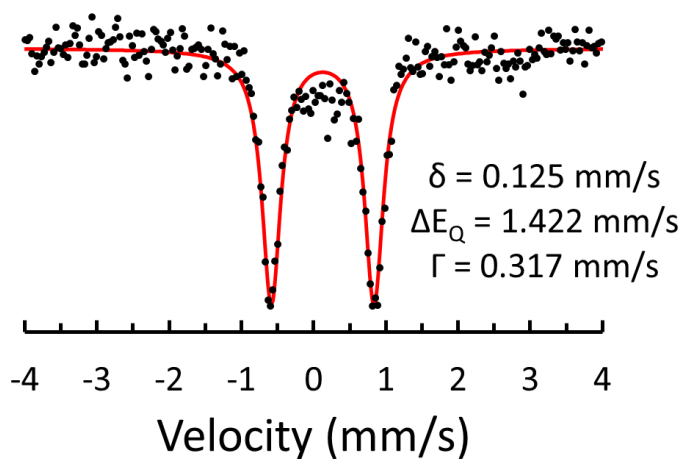


**Figure S17.** Zero field  $^{57}\text{Fe}$  Mössbauer spectra of solid **5'** collected at 80 K.

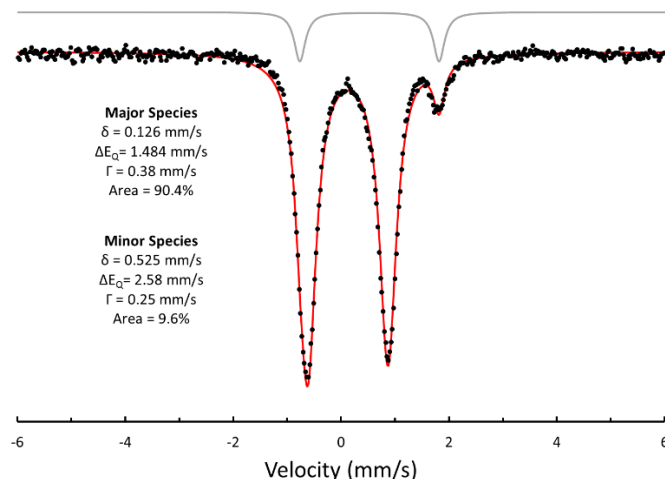


**Figure S18.** 80 K zero-field  $^{57}\text{Fe}$  Mössbauer spectrum of **5** in a frozen 2-MeTHF glass generated *in situ*. The spectrum was obtained by combining a 2-MeTHF solution of  $^{57}\text{Fe-1}$  (~5 mM) with a 2-MeTHF solution of  $\{\text{H}(\text{Et}_2\text{O})_2\} \{\text{BAR}^{\text{F}}_{24}\}$  (~25 mM) at  $-135 \text{ }^\circ\text{C}$ . The minor species is compound **3**.

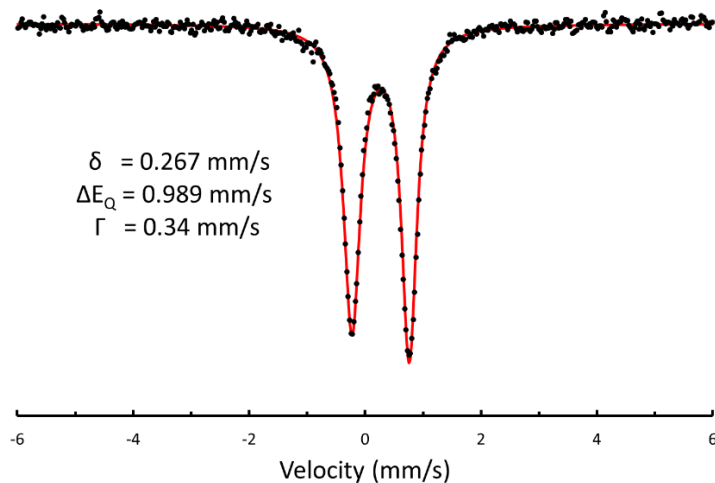


**Figure S19.** 80 K Zero-field  $^{57}\text{Fe}$  Mössbauer spectrum of  $^{57}\text{Fe-1}$  (~5 mM) in a frozen 2-MeTHF glass.

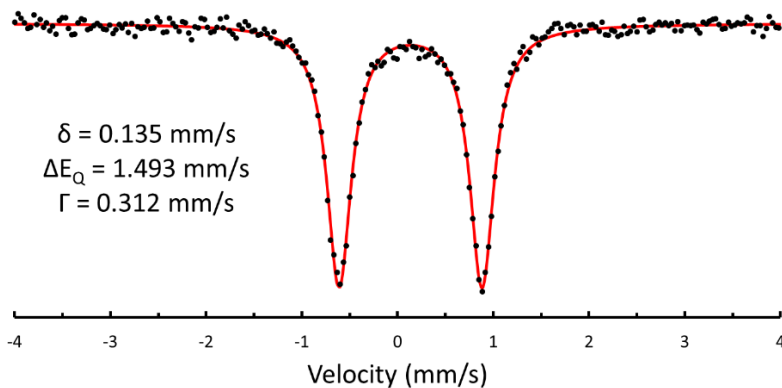


**Figure S20.** 80 K Zero-field  $^{57}\text{Fe}$  Mössbauer spectrum of solid **6**.

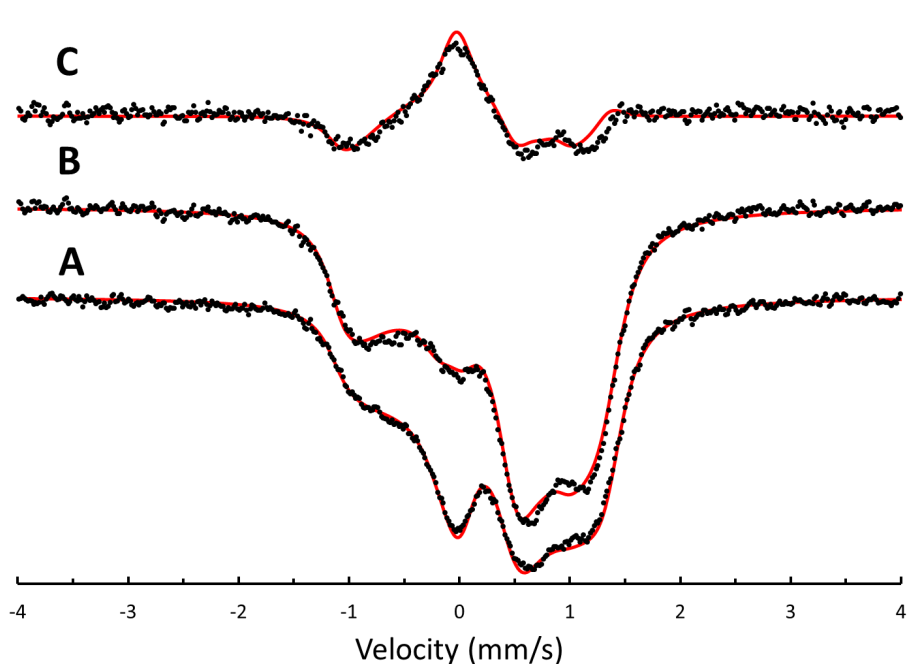


**Figure S21.** 5 K  $^{57}\text{Fe}$  Mössbauer spectra of a frozen 2-MeTHF solution of 5 mM  $\text{Fe}^{\text{I}}\text{-N}_2$  **2** in the presence of a 50 mT magnetic field oriented (A) perpendicular and (B) parallel to the propagation of the  $\gamma$ -beam. The difference spectrum (C) was obtained by subtracting the features of (A) from those of (B). Refer to Table S1 for the resulting fit parameters.

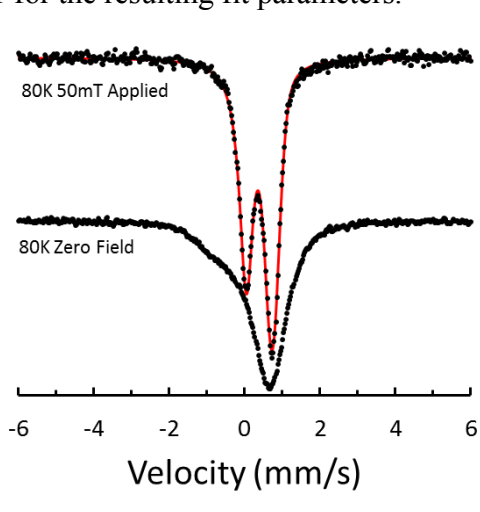


**Figure S22.** 80 K  $^{57}\text{Fe}$  Mössbauer spectra of a frozen 2-MeTHF solution of 5 mM **2** in the presence (top) or absence (bottom) of a 50 mT magnetic field applied parallel to the propagation of the  $\gamma$ -beam.

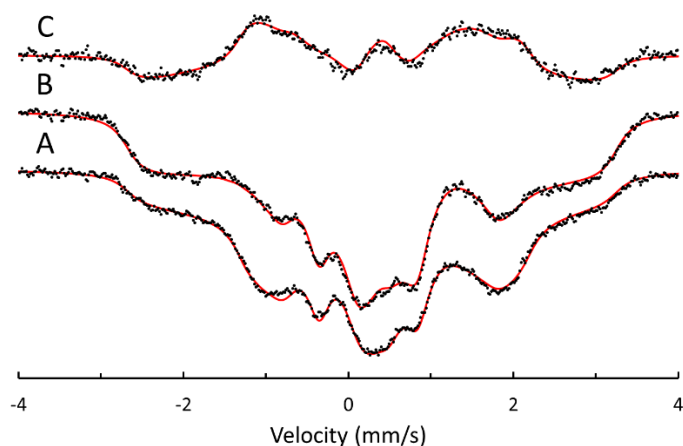


**Figure S23.** Raw 5 K  $^{57}\text{Fe}$  Mössbauer spectra of a frozen 2-MeTHF solution of 5 mM **8** in the presence of a 50 mT magnetic field oriented (A) perpendicular and (B) parallel to the propagation of the  $\gamma$ -beam. The difference spectrum (C) was obtained by subtracting the features of (A) from those of (B). The solid red lines represent best fits to the data by the simultaneous simulation of data in (A) and (B). Fit parameters for **8** are listed in Table S1.

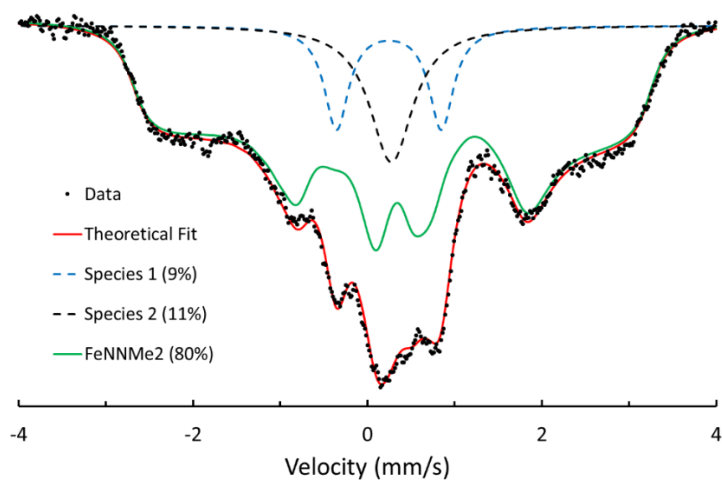


**Figure S24.** Spectral decomposition of the 5 K  $^{57}\text{Fe}$  Mössbauer spectra of a frozen 2-MeTHF solution of 5 mM **8** in the presence a 50 mT magnetic field applied parallel to the propagation of the gamma beam. Species 1 is characterized by a  $\Delta E_Q = 1.20$  and  $\delta = 0.24$  mm/s. Species 2 is characterized by a  $\Delta E_Q = 0.2$  and  $\delta = 0.28$  mm/s.

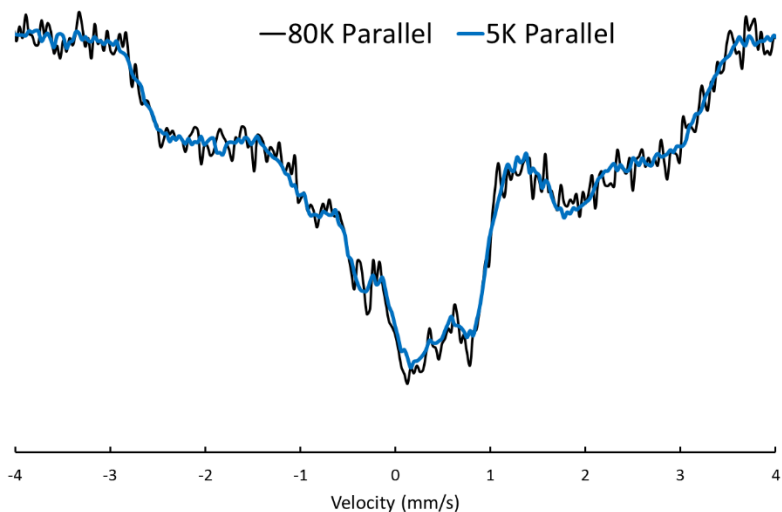


**Figure S25.**  $^{57}\text{Fe}$  Mössbauer spectra of a frozen 2-MeTHF solution of **8** in the presence of a 50 mT magnetic field applied parallel to the propagation of the gamma beam collected at 80 K (Black) and 5 K (Blue).

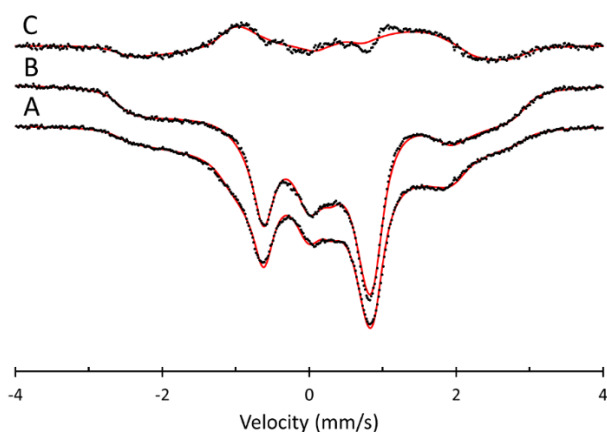


**Figure S26.** Raw 80 K  $^{57}\text{Fe}$  Mössbauer spectra of a frozen 2-MeTHF solution of 5 mM **7** in the presence of a 50 mT magnetic field oriented (A) perpendicular and (B) parallel to the propagation of the  $\gamma$ -beam. The difference spectrum (C) was obtained by subtracting the features of (A) from those of (B). The solid red line represent best fits to the data by the simultaneous simulation of data in (A) and (B). Fit parameters for **7** are listed in Table S1.

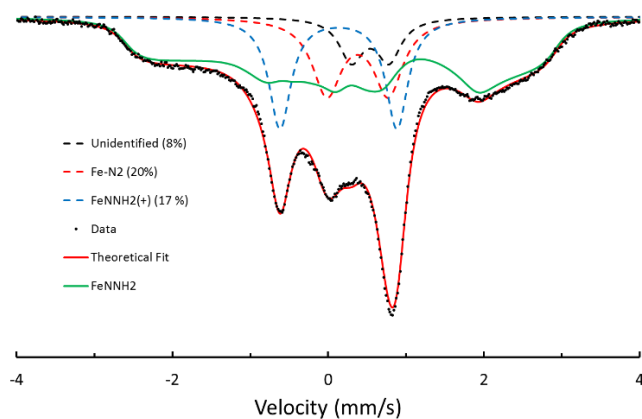


**Figure S27.** Spectral decomposition of the 80 K  $^{57}\text{Fe}$  Mössbauer spectra of a frozen 2-MeTHF solution of 5 mM **7** in the presence a 50 mT magnetic field applied parallel to the propagation of the gamma beam. Unreacted **5'** constitutes 17% of the spectrum. **2** constitutes 20% of the spectrum. An unidentified impurity constitutes 8% of the spectrum ( $\Delta E_Q = 0.49$  and  $\delta = 0.54$  mm/s) and the remainder is ascribed to **7** (55%, green).

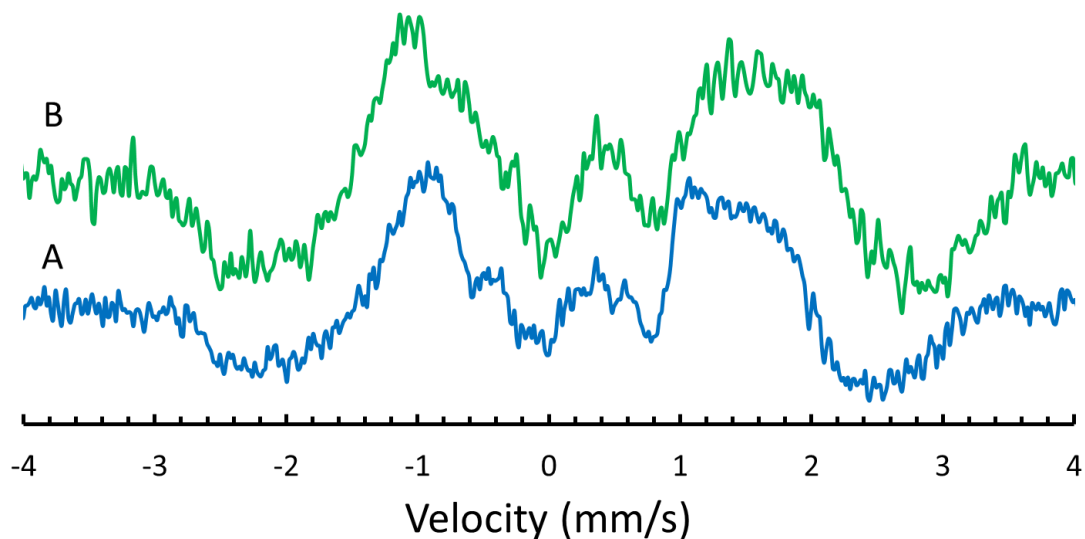


**Figure S28.** Comparison of the  $^{57}\text{Fe}$  Mossbauer difference spectra for **7** (A, bottom) and **8** (B, top) taken from Figures S32 and S29.

	<b>7</b>	<b>8</b>	<b>2</b>
$g_x$	2.070	2.080	2.400
$g_y$	2.027	2.030	2.000
$g_z$	2.004	2.000	2.000
$\Delta E_Q$ (mm/s)	0.856	0.898	0.674
$\delta$ (mm/s)	0.31	0.36	0.374
$\eta$	0.303	0.612	-1
$^{Fe}A_x$ (T)	33.1	35.9	14.8
$^{Fe}A_y$ (T)	7.4	8.8	4.8
$^{Fe}A_z$ (T)	14.6	12.8	0.3

**Table S1.** Best fit parameters derived from simulation of the magnetically-perturbed  $^{57}\text{Fe}$  Mössbauer spectra of **7**, **8** and **2**. The  $g$  values were obtained by EPR spectroscopy (see below).

### Supplemental Mossbauer Discussion

The magnetically-perturbed  $^{57}\text{Fe}$  Mössbauer spectra of **7** and **8** shown in the main text were obtained by subtraction of quadrupole doublet impurities from the raw data, and this procedure deserves some additional discussion. The raw experimental data for **8** (Figure S23) and **7** (Figure S26) are shown above. In order to observe the features ascribable to slow electronic relaxation, investigations of **8** were initially conducted at 5 K, a typical temperature for such studies, and the spectra of **8** shown in the main text derive from these studies. At this temperature, the simultaneous fitting of spectra (A) and (B) in Figure S23 suggested the presence of two quadrupole doublet impurities amounting to 20% of the [Fe] content (Figure S23). The identity of these impurities are unknown, but **8** is known to decompose in solution, and these impurities may be the products of that decomposition process. The features resulting from these impurities do not appear to be influenced by the orientation of a weak applied magnetic field.

Later studies (Figure S25) informed by EPR measurements (Figure S29) indicated that **8** displayed unusually-slow relaxation properties. As such,  $^{57}\text{Fe}$  Mössbauer data collected at 80 K displayed unquenched magnetic splitting: they are identical to that collected at 5 K. Collection of data at 80 K in these studies offers a number of advantages, most notably that rapidly-relaxing, EPR-active contaminants appear as quadrupole doublets, simplifying the interpretation of data. **2** is a consistent impurity found in preparations of **7**, as evidenced by EPR studies (Figure S30), and relaxes rapidly, rendering the 80 K Mossbauer spectrum of this complex to appear as a quadrupole doublet (Figure S21 and S22).

As EPR spectroscopy indicates that **7** and **8** have similar electronic structures, we assumed that **7** would display similar relaxation properties. Therefore the  $^{57}\text{Fe}$  Mössbauer spectra of **7** was collected at 80 K, (Figure S26). The spectra shown display features spread out over a similar range to that of **8** and their presence at this temperature are indicative of slow electronic relaxation. While samples containing **7** and **8** are contaminated with quadrupole-doublet impurities, the features associated with these impurities are not influenced by the orientation of the applied magnetic field, and thus the difference spectra (Figure S28) of these samples uniquely highlight the features ascribed to slowly-relaxing Fe species. These difference spectra are remarkable similar and reflect the presence of similar, slowly-relaxing EPR-active species in these preparations; namely **7** and **8**.

Using the difference spectra as a guide, along with the known parameters of **5'** and **2** at 80 K, the simulation of the spectra collected on the sample containing **7** is straightforward (Figure S27). Furthermore, since both **7** and **8** display features spread over a wide velocity range that extends past those of the impurities (Figure S27 and S24), initial fits focused on properly simulating the outer portions of the spectra. Taken together, the  $^{57}\text{Fe}$  Mössbauer studies conclusively indicate that an Fe-containing complex (**7**) that displays nearly identical parameters and physical properties to **8** (Table S1) is obtained upon chemical reduction of **5'**. This statement is bolstered by the EPR studies below.

## EPR Spectra

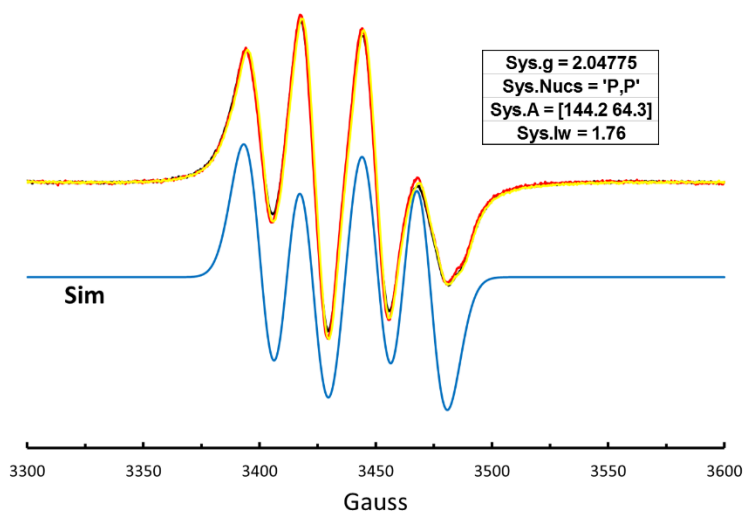


**Figure S29.** Overlaid 298 K X-band EPR spectra of **8** (black), **8-d<sub>6</sub>** (red), and  $^{15}\text{N}$ -**8** (yellow). The blue trace is derived from the simulation parameters listed in the table.

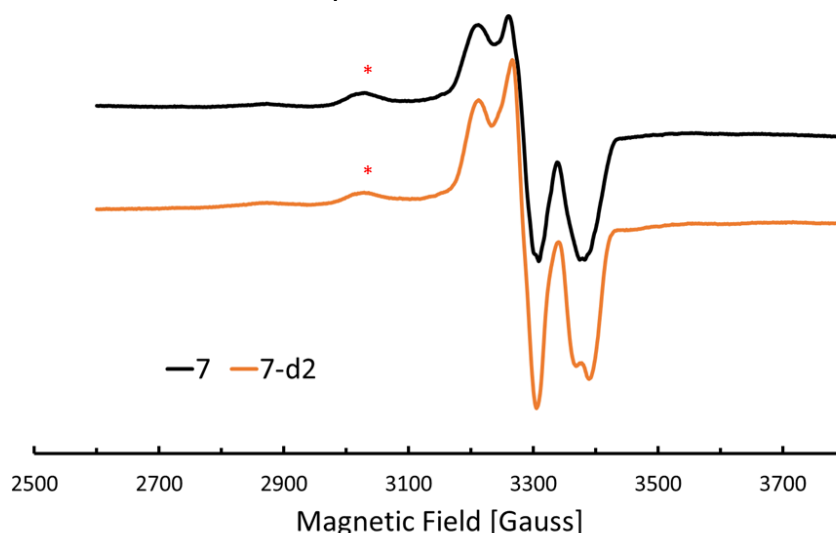


**Figure S30.** Raw EPR spectra of the reaction mixture obtained by addition of stoichiometric  $\text{Cp}^*\text{Co}$  to **5'** (black) and **5'-d<sub>2</sub>** (orange). The asterisk denotes a  $\text{Cp}^*\text{Co}$ -derived impurity.

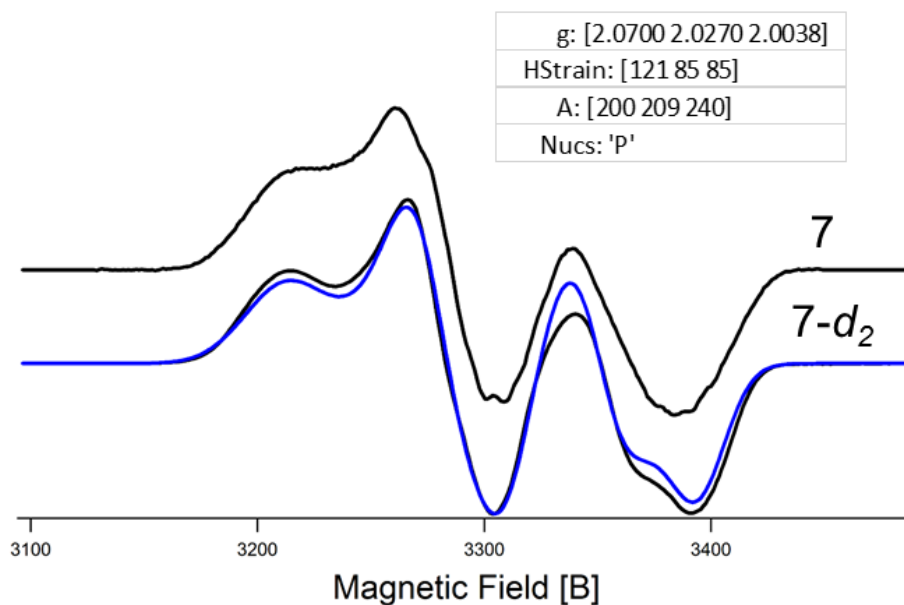


**Figure S31.** EPR spectra of **7** (top) and **7-d<sub>2</sub>** (bottom, black traces) and the best-fit simulation of **7-d<sub>2</sub>** (blue trace). (Inset) Simulation parameters used to generate the blue trace.

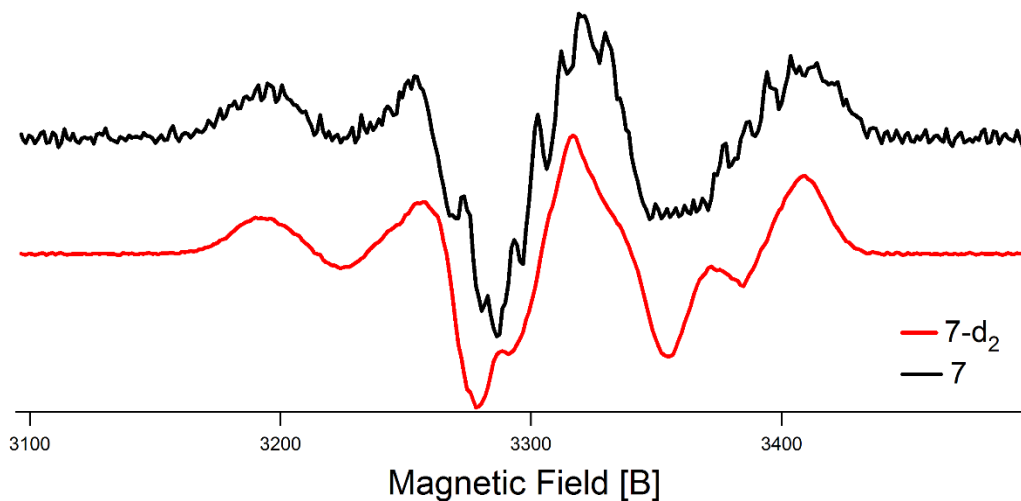


**Figure S32.** 2nd derivative of the EPR absorption envelope of **7** (top, black) and **7-d<sub>2</sub>** (bottom, red) collected at 77 K in a 2-MeTHF glass. The sharp features in the spectra of **7** display a relatively consistent spacing of ~25 MHz, placing a lower limit on the  $A(^1\text{H})$  for one or more of the  $\text{NNH}_2$  protons.

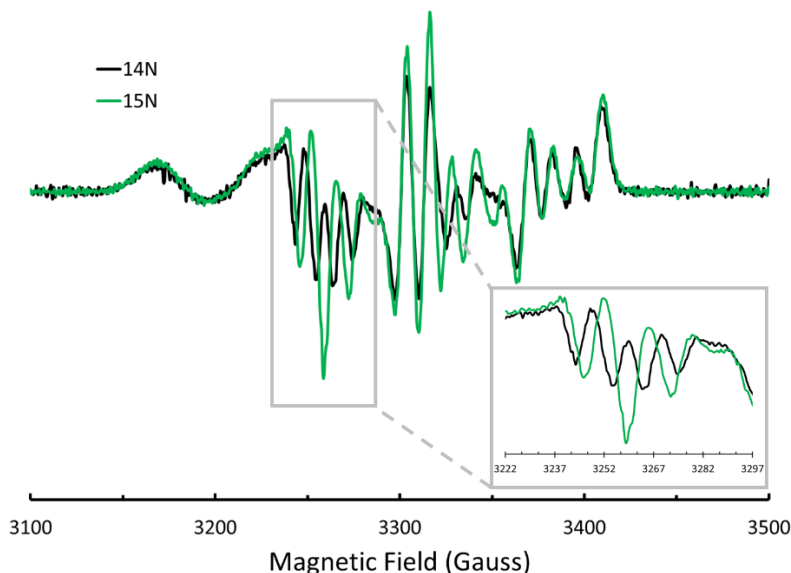


**Figure S33.** 2nd derivative of the EPR absorption envelope of **8** (black) and  $^{15}\text{N}$ -**8** (green) collected at 77 K in a 2-MeTHF glass. (Inset) region of greatest difference that highlights features arising from hyperfine coupling to one N-atom and one P-atom of similar magnitude. These features display spacings of  $\sim 28$  and  $\sim 37$  MHz for **8** and  $^{15}\text{N}$ -**8**, respectively, providing a crude estimate of the magnitude of the hyperfine coupling constants for these nuclei.

### Supplemental EPR Discussion

Compounds **7**, **8** and their isotopomers display rhombic EPR spectra centered around  $g = 2$  with small  $g$  anisotropy ( $\Delta g < 0.1$ ). These compounds display slow electronic relaxation, as evidenced by the  $^{57}\text{Fe}$  Mössbauer studies and the fact that **8** displays an intense EPR signal at elevated temperatures. At 298 K, the invariance in the spectra shown in Figure S29 indicate large hyperfine coupling to two chemically-inequivalent  $^{31}\text{P}$  nuclei. At 77 K, the small  $g$ -anisotropy and hyperfine coupling of this magnitude causes substantial overlap of the spectral features, hindering effective spectral simulations of the spectra shown in the main text. Additional, weaker hyperfine coupling to a third  $^{31}\text{P}$  nuclei as well as a single N atom are also observed. The nitrogen hyperfine coupling was conclusively assigned by comparison of the spectra of **8** and  $^{15}\text{N}$ -**8**. As shown in Figure 4A of the main text, four distinct features are observed in the region around  $g_2$  in **8** whereas only 3 distinct features are seen in  $^{15}\text{N}$ -**8**. In Figure S33, the 2<sup>nd</sup> derivative of the EPR absorption envelope of  $^{15}\text{N}$ -**8** and **8** are shown with an emphasis on the differing features.

For compound **7**, preparations employing  $\text{Cp}^*_2\text{Co}$  as a chemical reductant are invariably contaminated with an additional Co-derived impurity seen at 2950 Gauss that may arise from competing protonation of  $\text{Cp}^*_2\text{Co}$  ( $\text{Cp}^*_2\text{Co}$  is completely consumed in these reaction, by comparison to an authentic sample). This feature is observed in low and varying intensities from sample to sample and therefore is not considered to be a component of the EPR spectrum of **7**, although additional features from this impurity may be present at the same fields as those of **7**. (Figure S30). Compound **2** is also observed in each spectra, but its contribution can be effectively removed since this complex displays a feature at 2850 Gauss, which is well separated from those ascribable to **7**, and its authentic spectrum is known.<sup>1</sup>

Compound **7** and **7-d<sub>2</sub>** consistently display significant differences from each other in each sample examined. Overall, **7-d<sub>2</sub>** exhibits smoother features, and is noticeably distinct from **7** at the

highest magnetic fields. **7-d<sub>2</sub>** can be effectively simulated with a simple model that includes large hyperfine coupling to a single <sup>31</sup>P nuclei (Figure S31). The broad nature of the lineshape required to simulate the spectrum indicates substantial hyperfine coupling to other nuclei (and possibly some amount of g-Strain). In natural-abundance **7**, some of this hyperfine coupling is partially resolved as seen in Figure S31, but is more clearly seen in the 2<sup>nd</sup> derivative EPR spectrum (Figure S32). While we have not yet been able to effectively simulate the spectrum of **7**, the difference in linewidths observed between **7** and **7-d<sub>2</sub>** and the features present in the 2<sup>nd</sup> derivative spectra (Figure S32) imply hyperfine coupling constants of approximately 25 MHz to one or more hydrogen atoms. In depth EPR and ENDOR studies on these complexes will be reported in due course.

## X-Ray Diffraction Data

Compound	1	5	5'	6	8
Chem formula	C <sub>40</sub> H <sub>63</sub> FeKN <sub>2</sub> OP <sub>3</sub> Si	C <sub>76</sub> H <sub>85</sub> BF <sub>24</sub> FeN <sub>2</sub> O <sub>2</sub> P <sub>3</sub> Si	C <sub>46</sub> H <sub>68</sub> F <sub>3</sub> FeN <sub>2</sub> O <sub>5</sub> P <sub>3</sub> SSi	C <sub>39</sub> H <sub>60</sub> F <sub>3</sub> FeN <sub>2</sub> O <sub>3</sub> P <sub>3</sub> SSi	C <sub>38</sub> H <sub>60</sub> FeN <sub>2</sub> P <sub>3</sub> Si
fw	803.87	1705.72	988.27	870.8	721.73
cryst syst	Triclinic	Triclinic	Monoclinic	Orthorhombic	Triclinic
Space group	P-1	P-1	C2/C	Pna2 <sub>1</sub>	P-1
a [Å]	10.3640(4)	12.9079(7)	27.371(3)	20.9744(9)	10.3195(9)
b [Å]	10.9643(4)	16.5462(9)	12.5437(11)	14.6729(7)	10.8239(10)
c [Å]	18.9571(8)	19.6878(12)	31.967(3)	13.7649(8)	19.3470(17)
α [°]	88.362(2)	75.755(3)	90	90	78.665(5)
β [°]	84.430(2)	77.192(3)	108.726(3)	90	78.078(5)
γ [°]	18.9571(8)	78.758(3)	90	90	62.522(4)
V [Å <sup>3</sup> ]	2129.46(14)	3930.1(4)	10394.2(16)	4236.2(4)	1963.1(3)
Z	2	2	8	4	2
D <sub>calcd</sub> [g cm <sup>-3</sup> ]	1.254	1.441	1.263	1.365	1.287
F(000)	858	1758	4179	1840	774
μ [mm <sup>-1</sup> ]	5.287	0.372	0.499	0.599	0.595
temp [K]	100	100	100	100	100
wavelength [Å]	1.54178	0.71073	0.71073	0.71073	0.71073
measured reflns	56751	241133	111268	43639	94112
unique reflns	8734	20816	10643	10510	11387
data/restraints/param	8671/12/467	20771/6/1158	10622/39/628	10256/19/561	11386/0/420
R(F) (I>2σ(I))	0.0607	0.0437	0.0424	0.0321	0.0269
wR(F <sup>2</sup> )(all)	0.1502	0.1256	0.109	0.0786	0.071
GOOF	1.03	1.077	1.051	1.061	1.029

**Table S2.** X-ray diffraction table.

### Remarks on the Crystal Structure of Compound 1

The crystal structure of **1** is of high quality but suffers from disordered methyl groups within the (iPr)<sub>2</sub>P portion of the [SiP<sup>iPr</sup><sub>3</sub>] ligand. This disorder gives rise to 3 Level C Alerts in the CheckCif report.

### Remarks on the Crystal Structure of Compound 5

The crystal structure of **5** is of high quality but suffers from disorder in three regions. Overall, these regions of disorder do not noticeably influence the Fe=NNH<sub>2</sub><sup>(+)</sup> unit, which is highly-ordered. One of the (iPr)<sub>2</sub>P groups is disordered over two positions in a ratio of 85:15. In the minor component, one of the methyl groups is unusually prolate and its anisotropic modeling resulted in the appearance of a single level B Alert (PLAT213\_ALERT\_2\_B Atom C80B) in the CheckCif report.

A second region of disorder is near one of the ethereal molecules that are hydrogen bonding to the NNH<sub>2</sub> protons. At this site, one of these Et<sub>2</sub>O molecules is substituted by a 2-methyltetrahydrofuran molecule in 30% of the crystal.

A final region of disorder is found among the CF<sub>3</sub> groups of the BAr<sup>F</sup><sub>24</sub> counteranion. This disorder was partially modelled but nonetheless resulted in the appearance of a few level C Alerts.

### Remarks on the Crystal Structure of Compound 5'

The crystal structure of **5'** is of high quality but suffers from heavily disordered cocrystallized solvent molecules. A 2-methyltetrahydrofuran is found to be disordered over a special position and a tetrahydrofuran molecule was modeled as occupying two positions in a ratio of 60:40. Despite our best attempts to properly model this disorder, a number of Level C Alerts arise in the CheckCif

report as a consequence of this disorder. This disorder is not extended to the  $[\text{SiP}_3]\text{Fe}=\text{NNH}_2^{(+)}$  or  $\text{OTf}^{(-)}$  fragments, both of which are highly-ordered.

#### Remarks on the Crystal Structure of Compound 6

The crystal structure of **6** is of high quality but suffers from a disordered  $(\text{iPr})_2\text{P}$  group and a racemic twin. The  $(\text{iPr})_2\text{P}$  group is disordered over two slightly-different orientations in a ratio of 68:32. Anisotropic modeling of the minor component leads to appearance of 3 Level C Alerts in the CheckCif report.

The crystal was additionally found to contain a racemic twin in a ratio of 75:25 for the two configurations.

#### Remarks on the Crystal Structure of Compound 8

The crystal structure of **8** is of exceptional quality.

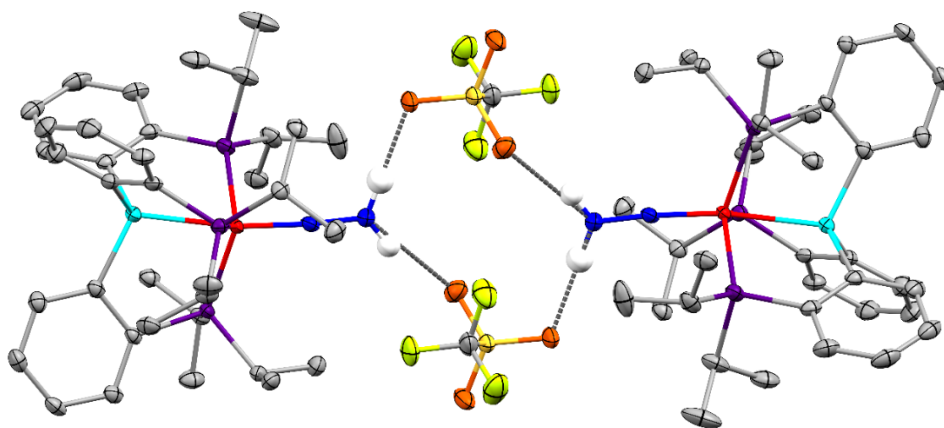


**Figure S34.** Expanded view of the XRD structure of **5'** illustrating the hydrogen bond network within the crystal lattice.

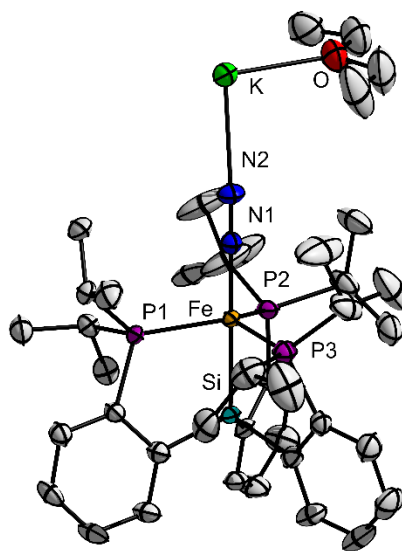


**Figure S35.** X-ray diffraction crystal structure of **1** with thermal ellipsoids drawn at 50% probability.

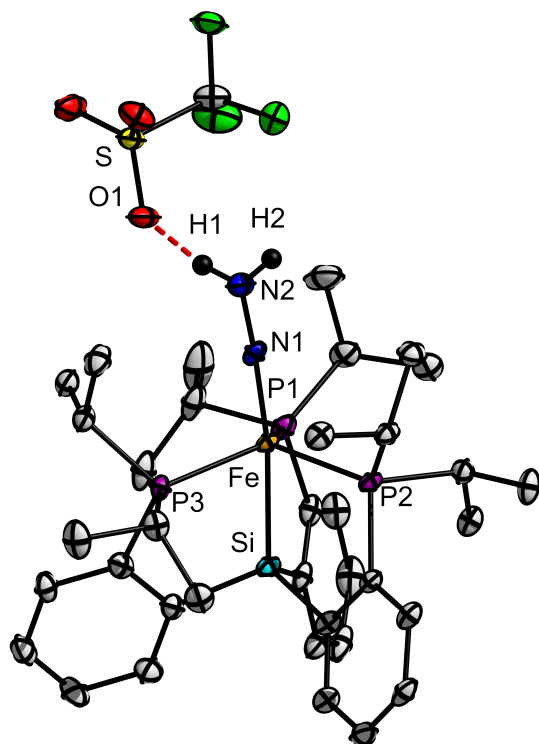


**Figure S36.** X-ray diffraction crystal structure of **5'** with thermal ellipsoids drawn at 50% probability. Cocrystallized solvent molecules have been removed for clarity.

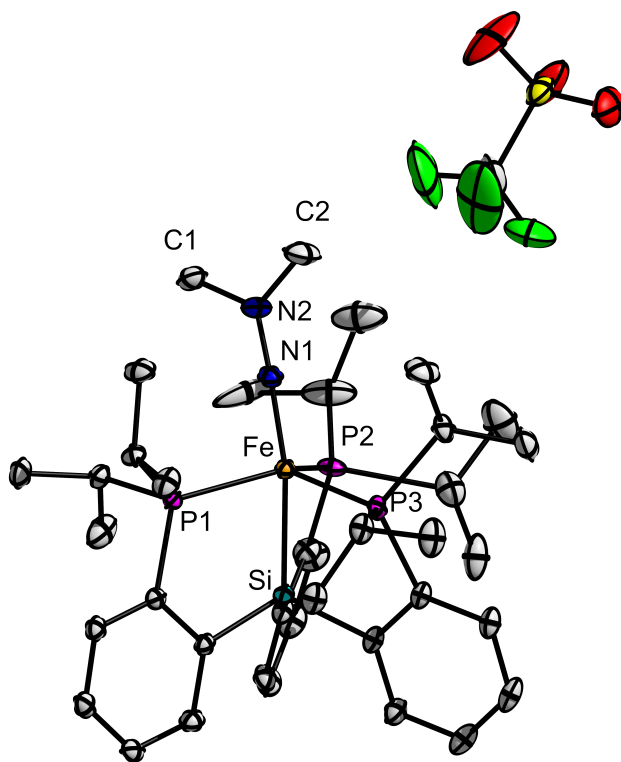


**Figure S37.** X-ray diffraction crystal structure of **6** with thermal ellipsoids drawn at 50% probability.

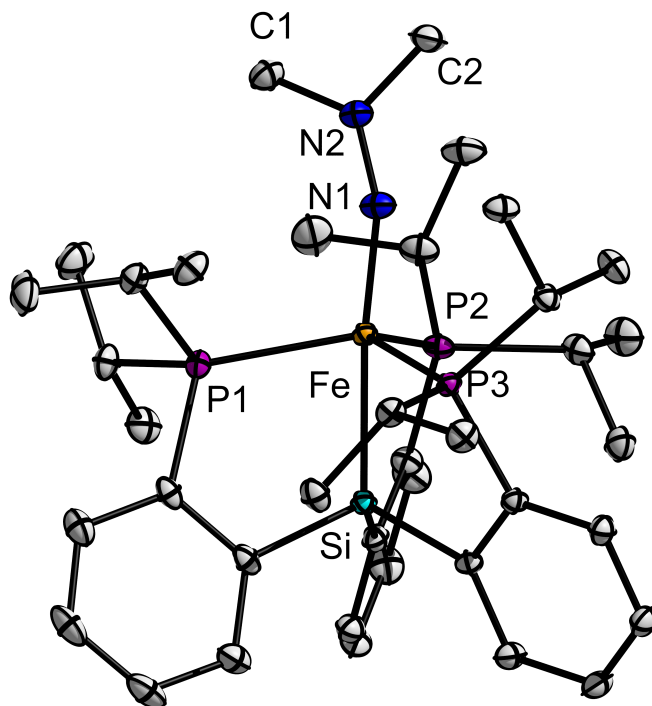


**Figure S38.** X-ray diffraction crystal structure of **8** with thermal ellipsoids drawn at 50% probability.

### DFT Calculations

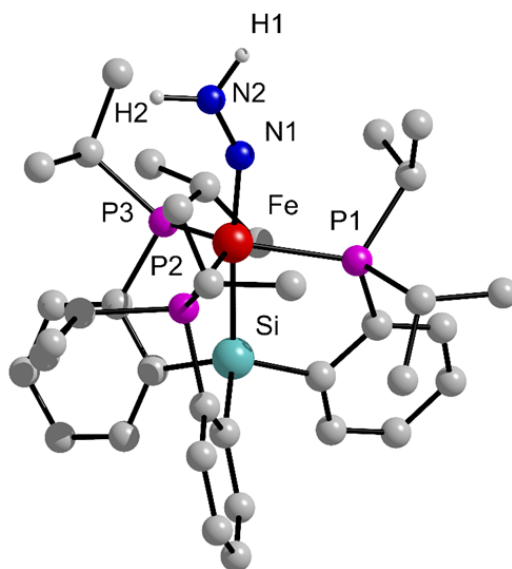


**Figure S39.** Gas-phase optimized geometry of **7** (Charge = 0,  $S = 1/2$ ). Fe-N(1): 1.747 Å, N(1)-N(2): 1.294 Å, Fe-P(1): 2.335 Å, Fe-P(2): 2.276 Å, Fe-P(3): 2.276 Å, Fe-Si: 2.333 Å, Si-Fe-N(1): 175.3°, Fe-N(1)-N(2): 150.6°.

	<b>7<sup>a</sup></b>	<b>8<sup>a</sup></b>	<b>8<sup>b</sup></b>
Fe-N <sup>c</sup>	1.7468	1.7705	1.773(1)
Fe-Si <sup>c</sup>	2.3333	2.3318	2.3021(5)
Fe-P1 <sup>c</sup>	2.2762	2.2883	2.2700(3)
Fe-P2 <sup>c</sup>	2.2762	2.2963	2.2989(4)
Fe-P3 <sup>c</sup>	2.3349	2.3514	2.3182(4)
N-N <sup>c</sup>	1.2941	1.2828	1.276(2)
Si-Fe-N <sup>d</sup>	175.29	174.97	174.20(4)
Fe-N-N <sup>d</sup>	150.58	158.11	158.64(9)
P1-Fe-P2 <sup>d</sup>	118.58	120.38	118.13(1)
P2-Fe-P3 <sup>d</sup>	114.78	111.858	112.83(1)
P1-Fe-P3 <sup>d</sup>	116.99	117.65	119.21(1)

**Table S3.** Comparison of pertinent bond metrics. <sup>a</sup>DFT-optimized geometry (gas-phase). <sup>b</sup>X-ray diffraction crystal structure (solid state). <sup>c</sup> Reported in Angstroms. <sup>d</sup> Reported in degrees.

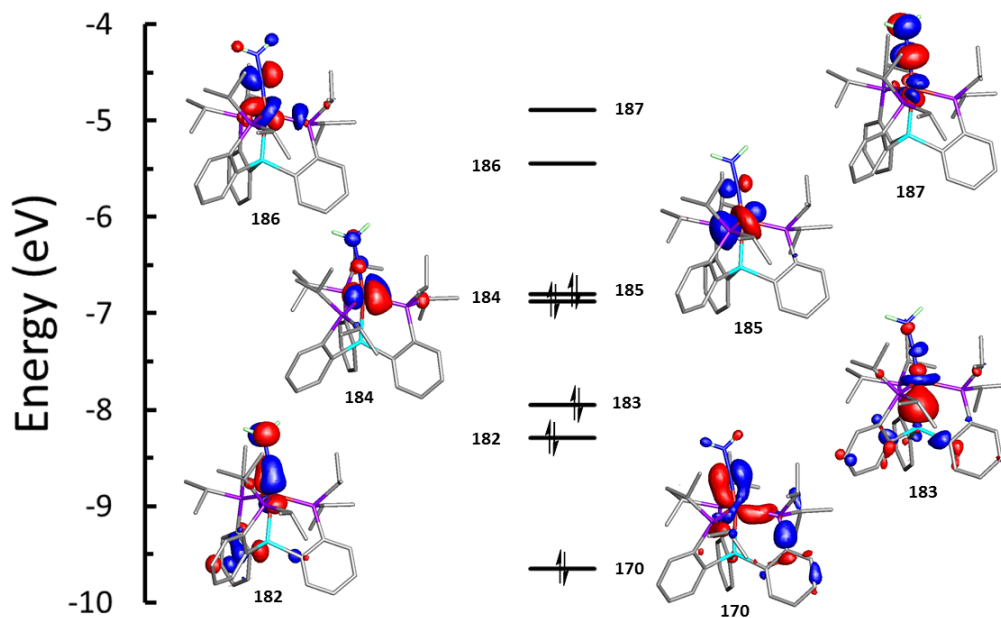


**Figure S40.** Frontier molecular orbitals of  $[\text{SiP}^{\text{iPr}}_3]\text{Fe}=\text{NNH}_2^{(+)}$  ( $S = 0$ ). Contour values set to  $0.05 \text{ \AA}^3$ .

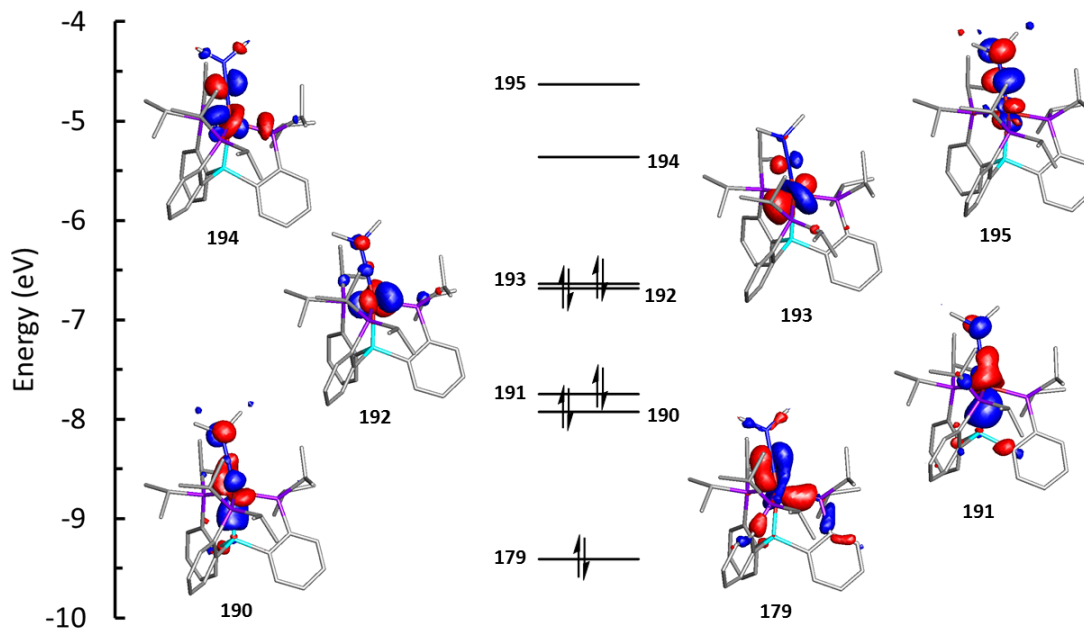


**Figure S41.** Frontier molecular orbitals of  $[\text{SiP}^{\text{iPr}}_3]\text{Fe}=\text{NNMe}_2^{(+)}$  ( $S = 0$ ). Contour values set to  $0.05 \text{ \AA}^3$ .

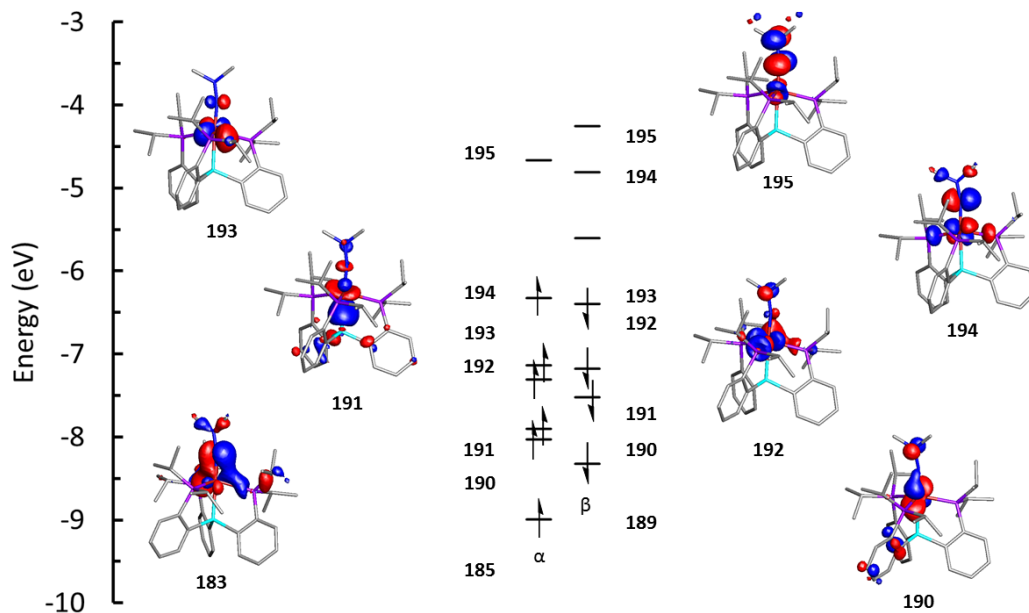


**Figure S42.** Frontier molecular orbitals of **8**. Orbitals shown correspond to the  $\alpha$  manifold. Contour values set to  $0.05 \text{ \AA}^3$ .

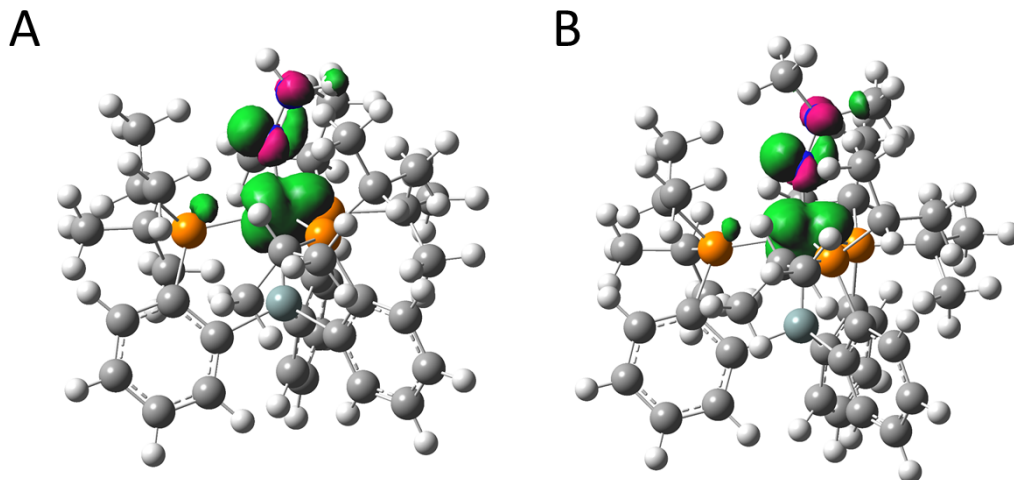


**Figure S43.** Spin density plots of Fe=NNH<sub>2</sub> **7** (A) and Fe=NNMe<sub>2</sub> **8** (B) with contour values set to 0.03 Å<sup>3</sup>.

**Optimized Coordinates for [SiP<sup>iPr</sup><sub>3</sub>]Fe=NNH<sub>2</sub> (Charge = 1+, S = 0)**

Fe	-0.04695600	0.03682800	-1.05672300
P	2.05968700	-0.97722400	-0.67922100
P	0.03839300	2.21669700	-0.53975800
P	-2.12369100	-0.89089000	-0.62850900
Si	0.01293400	-0.08645900	1.31452200
N	-0.14074400	-0.19493400	-2.70381000
N	-0.24486300	-0.46753000	-3.96017900
C	0.97089600	3.23669900	-1.82236900
C	-2.36837200	2.86037100	0.84165000
C	2.44632800	2.85522600	-1.99788100
C	1.36595800	3.84086600	1.45744900
C	1.84241600	4.02201300	2.76663800
C	1.13986600	-1.51678200	1.85492600
C	1.44201600	-3.26954900	-2.30694800
C	-1.58157300	3.20733300	-0.43506200
C	-1.42955000	4.74138600	-0.52767400
C	-1.69926700	-0.44081500	2.05157800
C	0.69256000	1.54345600	2.02254200
C	0.79187000	2.60677500	1.08724000
C	3.74173400	-0.08189300	-0.48371300
C	2.51577900	-2.20462600	-2.03601700
C	2.02464500	-1.99433300	0.85571700
C	-2.68505100	-0.84721100	1.11977800
C	0.25393500	3.23495100	-3.18543300
C	3.81102900	0.75524300	0.80450800
C	1.16566400	1.75285700	3.33502600
C	-4.34589900	0.93053600	-1.15983400
C	-2.05442800	-2.75564200	-1.02971300

H	-1.45421200	-2.79201700	-1.95854800
C	2.83181300	-3.12636500	1.10059200
C	1.73490500	2.98271300	3.70648300
C	-2.04756900	-0.36194300	3.41743600
C	-1.29547500	-3.51906900	0.07159500
H	-1.87610900	-3.53690600	1.01026600
H	-1.13989500	-4.56625400	-0.24646800
H	-0.31149100	-3.07994900	0.29442800
C	2.76822400	-3.77688200	2.34402500
C	4.97761300	-1.00720500	-0.53622000
C	-3.67928800	-0.38580700	-1.58757700
C	-3.98594000	-1.18452600	1.55385300
C	-3.34242800	-0.69210800	3.84926800
C	1.10063300	-2.17704000	3.10116500
C	1.91171300	-3.29685400	3.34834400
C	-4.30895700	-1.10882100	2.91791500
C	2.97883300	-1.50798800	-3.33146800
C	-3.40383500	-3.45565800	-1.29492000
H	-3.93364400	-3.07473500	-2.18320500
H	-3.21323900	-4.53107300	-1.46828700
H	-4.07996600	-3.38968300	-0.42365400
C	-3.46177900	-0.41025600	-3.11021700
H	1.12372400	0.94071300	4.07136200
H	2.11146600	3.12673400	4.72524000
H	2.30278100	4.97452400	3.05076300
H	1.46509100	4.65787900	0.73401600
H	-1.31148900	-0.01611000	4.15352700
H	-3.60240800	-0.61686200	4.91091600
H	-5.32050700	-1.36386700	3.25184100
H	-4.75786700	-1.49108900	0.83955100
H	0.40578000	-1.83873700	3.87907500
H	1.86147000	-3.80795400	4.31614800
H	3.38545000	-4.66373200	2.52410800
H	3.49921300	-3.52465800	0.32901500
H	1.18190100	-3.83550400	-1.39717000
H	0.51097700	-2.82325400	-2.69698300
H	1.81520200	-3.99005100	-3.05818000
H	3.38919200	-2.73423100	-1.61259400
H	2.17731900	-0.90294800	-3.78368800
H	3.28017700	-2.27284000	-4.07131100
H	3.84793200	-0.84855400	-3.17191400
H	3.01562000	1.50949200	0.86874900
H	3.74426400	0.11492600	1.70141200
H	4.78257700	1.28155400	0.84253100
H	4.97546600	-1.73301200	0.29510500
H	5.09165500	-1.55548000	-1.48487600

H	5.88168000	-0.38221900	-0.41530300
H	3.78187700	0.59999300	-1.35138300
H	2.53796900	1.85835200	-2.46253200
H	2.99592000	2.85476000	-1.04223900
H	2.93882600	3.58303700	-2.66919400
H	0.93004800	4.26226800	-1.40891400
H	-0.81023700	3.51817600	-3.12390000
H	0.75172600	3.94614700	-3.86959400
H	0.31721700	2.23252100	-3.64350800
H	-2.15400700	2.86157500	-1.31634000
H	-2.50108600	1.77716000	0.98264400
H	-3.37082400	3.32324200	0.79534100
H	-1.85768100	3.25550100	1.73669500
H	-2.42908300	5.20055500	-0.41453600
H	-0.80190900	5.13676500	0.29046000
H	-1.02011500	5.09176200	-1.48892100
H	-5.33315600	1.00855300	-1.65203100
H	-4.50794100	0.99027500	-0.07217500
H	-3.75654100	1.80681000	-1.47307900
H	-4.38327600	-1.19904000	-1.32986900
H	-2.80533000	0.41922800	-3.42397100
H	-3.01578800	-1.35541900	-3.46621900
H	-4.43080600	-0.28449700	-3.62726200
H	-0.38091200	0.28131700	-4.64967300
H	-0.33394500	-1.43607600	-4.29001900

**[SiP<sup>iPr</sup><sub>3</sub>]Fe=NNMe<sub>2</sub> (Charge = 1+, S = 0)**

Fe	0.24952200	-0.70024100	0.51382200
P	-1.81466000	-1.46382500	-0.38563000
P	-0.24230100	0.88067100	2.06928500
P	2.25519800	-0.26258600	-0.60069200
Si	-0.38683200	1.09566400	-0.91212100
N	0.86734800	-2.11902100	1.19860900
N	1.44780200	-3.14454500	1.70617600
C	-1.05470600	0.34996700	3.69515800
C	1.71387300	2.92019000	1.74860900
C	-2.50897300	-0.13353500	3.61265500
C	-2.02536900	3.14748200	2.31788600
C	-2.77363500	4.19011200	1.74789800
C	-1.51370800	0.48714000	-2.31117600
C	-0.76468900	-3.76602800	-1.73657200
C	1.25346700	1.84959400	2.75548300
C	1.07513300	2.52168700	4.13413700
C	1.09664700	1.96422900	-1.71503700
C	-1.35293900	2.40213300	0.07680500

C	-1.31663400	2.25420900	1.48540700
C	-3.53007900	-1.26608600	0.43796700
C	-1.82202700	-3.32051300	-0.71459000
C	-2.13905500	-0.75758200	-2.05885100
C	2.33840300	1.30531400	-1.55826700
C	-0.21276500	-0.66996600	4.47640600
C	-4.03613800	0.18546300	0.35239000
C	-2.11079300	3.45714200	-0.47534000
C	4.34910200	0.90266400	1.07437200
C	2.48192500	-1.58490300	-1.96159500
H	2.20377700	-2.52577000	-1.45005500
C	-2.97150000	-1.34697800	-3.03563500
C	-2.81506300	4.34700400	0.35182300
C	1.05521300	3.17293500	-2.44404300
C	1.49304100	-1.34311900	-3.11715400
H	1.77285000	-0.44218300	-3.69026300
H	1.51640500	-2.20361800	-3.81061400
H	0.45680000	-1.21149800	-2.77071400
C	-3.18542600	-0.69482500	-4.26081900
C	-4.64413700	-2.20425300	-0.07534700
C	3.97088600	-0.31198400	0.21202600
C	3.51103800	1.84201100	-2.13509900
C	2.22017500	3.70796200	-3.01637500
C	-1.74411700	1.12900500	-3.54677000
C	-2.57658200	0.54545100	-4.51547100
C	3.44681600	3.03937800	-2.86479000
C	-1.79425900	-4.13385000	0.59200800
C	3.90328200	-1.74284100	-2.53965200
H	4.64945300	-2.08258700	-1.80282600
H	3.87433800	-2.50040900	-3.34475100
H	4.26172600	-0.80435900	-2.99890800
C	4.24502000	-1.61592300	0.97802500
H	-2.18077900	3.57169500	-1.56412100
H	-3.40818100	5.15518200	-0.09041000
H	-3.33159700	4.87552600	2.39514700
H	-2.01637300	3.03385900	3.40743500
H	0.11116100	3.72139800	-2.54689000
H	2.17562300	4.65131700	-3.57179700
H	4.35894800	3.45621900	-3.30542000
H	4.48068100	1.34787600	-2.01276900
H	-1.24761900	2.08039900	-3.77182300
H	-2.73874700	1.04854100	-5.47522500
H	-3.82163900	-1.16215500	-5.02034400
H	-3.44317700	-2.32059100	-2.86551900
H	-0.95090800	-3.32337000	-2.72874200
H	0.25238200	-3.46971500	-1.43386400

H	-0.78748900	-4.86622100	-1.84717700
H	-2.80809400	-3.48988700	-1.18492700
H	-0.87444100	-3.95082100	1.16838000
H	-1.84863600	-5.21444000	0.36381100
H	-2.64701000	-3.89207700	1.24964100
H	-3.30973900	0.91891600	0.72863700
H	-4.27854200	0.45719700	-0.68991100
H	-4.96239200	0.28506800	0.94775500
H	-4.85989700	-2.03786100	-1.14497700
H	-4.44037900	-3.27550600	0.08362900
H	-5.57308100	-1.96930100	0.47678300
H	-3.33792500	-1.51252800	1.49580200
H	-2.56174800	-1.15535000	3.20114800
H	-3.14815800	0.52860500	3.00725800
H	-2.93617600	-0.17328600	4.63210800
H	-1.05620600	1.29923500	4.26205000
H	0.85076900	-0.38461800	4.55814200
H	-0.60865700	-0.77635300	5.50333100
H	-0.27319500	-1.65942900	3.99348900
H	2.03622600	1.07255900	2.84276300
H	1.84000100	2.52830200	0.72821900
H	2.68191800	3.34287800	2.07298700
H	0.98512600	3.74759000	1.70192500
H	2.00009200	3.07845900	4.37406400
H	0.25437300	3.26109600	4.12200300
H	0.90107100	1.81406000	4.96047300
H	5.42658700	0.84736800	1.31785800
H	4.17018700	1.85968800	0.56010600
H	3.80052100	0.91309900	2.03041300
H	4.63669500	-0.29736000	-0.67063400
H	3.65899900	-1.65031400	1.91150500
H	4.01316900	-2.51751700	0.38527500
H	5.31399700	-1.66641500	1.25578600
C	1.81015100	-3.20124900	3.13410800
H	1.05713400	-3.77975100	3.70116900
H	2.79052400	-3.69788800	3.23359000
H	1.86822300	-2.17949900	3.52874600
C	1.79010300	-4.35057200	0.93158200
H	2.88630100	-4.49263800	0.92991100
H	1.31891100	-5.23588700	1.39577400
H	1.42417800	-4.23807000	-0.09504300

**[SiP<sup>iPr</sup><sub>3</sub>]Fe=NNH<sub>2</sub> (Charge = 0, S = 1/2)**

Fe	0.26930900	-0.39822500	-0.74095100
P	-0.81576500	-2.13248700	0.28435800

P	2.27538400	0.36262500	0.07732700
P	-1.23578900	1.19419600	-1.59406900
Si	-0.43496900	0.66804200	1.20952300
N	0.87532700	-1.07509800	-2.26051800
N	1.45742000	-1.90681400	-3.04479200
C	3.85243300	-0.67720900	-0.13235900
C	2.11104900	3.22224200	-0.12823300
C	3.74785900	-2.07344600	0.49721000
C	3.42392500	0.74149300	2.73562500
C	3.28944600	1.01336400	4.10780400
C	-1.78338800	-0.31804600	2.13235500
C	-3.19828500	-2.67782600	-1.26511700
C	2.98978500	2.03594000	-0.55540100
C	4.44928000	2.35966900	-0.16951000
C	-1.11083500	2.42518400	0.85890900
C	0.99316000	0.88501100	2.45933100
C	2.28228000	0.67655200	1.90721800
C	0.27930300	-3.41705700	1.20977400
C	-1.93511500	-3.33212400	-0.68902800
C	-1.96619500	-1.64305900	1.66180000
C	-1.36343100	2.69363800	-0.51361600
C	4.32331400	-0.75171100	-1.59703300
C	0.85020300	-2.79968700	2.49971100
C	0.87983500	1.16644400	3.83751100
C	0.64676600	2.35680800	-3.40893900
C	-3.11962500	0.91136300	-1.86842800
H	-3.15288100	-0.03454200	-2.44083300
C	-2.95493400	-2.46707800	2.24310900
C	2.01706300	1.23137100	4.66006700
C	-1.25254700	3.47556600	1.79001800
C	-3.85405300	0.70108200	-0.53367900
H	-3.91088800	1.64577800	0.03563900
H	-4.89000800	0.36023700	-0.72306700
H	-3.36153000	-0.04198500	0.10979500
C	-3.75897100	-1.98192100	3.28823700
C	-0.33628700	-4.79062300	1.54453600
C	-0.80732900	1.87015300	-3.31068900
C	-1.71713800	3.99457200	-0.92896600
C	-1.61105800	4.77021500	1.37544700
C	-2.59981700	0.15094500	3.18434800
C	-3.58112200	-0.67154300	3.76193600
C	-1.83079700	5.03170400	0.01339000
C	-1.18373400	-4.06783400	-1.80858500
C	-3.87344000	1.99143200	-2.67214700
H	-3.49103700	2.13808500	-3.69588800
H	-4.93751600	1.69752900	-2.76114500

H	-3.85040700	2.96450600	-2.15021900
C	-1.11632400	0.81858200	-4.39538900
H	-0.11197200	1.30411100	4.28645500
H	1.91086200	1.43534200	5.73235400
H	4.18079600	1.04627100	4.74544300
H	4.42614200	0.56314400	2.33021400
H	-1.04147100	3.29561400	2.85202700
H	-1.69760800	5.57934600	2.11069300
H	-2.08669700	6.04469900	-0.31928000
H	-1.88407900	4.21821200	-1.98901600
H	-2.49224600	1.18393500	3.53973000
H	-4.21616500	-0.28843200	4.56981200
H	-4.53124200	-2.62602400	3.72526700
H	-3.12362000	-3.48592600	1.87642700
H	-3.79224500	-2.15855600	-0.49627900
H	-2.93749100	-1.95125400	-2.05285300
H	-3.84178300	-3.45243900	-1.72608000
H	-2.25790400	-4.08274300	0.05642000
H	-0.84067100	-3.35185700	-2.57564800
H	-1.85737700	-4.79499700	-2.30204800
H	-0.30667800	-4.62638300	-1.43964900
H	1.28057800	-1.80011400	2.33317000
H	0.06187600	-2.69930100	3.26671100
H	1.64243000	-3.45216800	2.91410100
H	-1.20650200	-4.68875200	2.21773800
H	-0.64878500	-5.36525100	0.65652500
H	0.41377800	-5.40330800	2.08180800
H	1.12047000	-3.57984300	0.50789500
H	2.96890400	-2.67923000	0.00574800
H	3.50535900	-2.02026100	1.57152900
H	4.71069500	-2.61036900	0.39187300
H	4.62560800	-0.12435300	0.43293100
H	4.50048100	0.24402600	-2.03727200
H	5.27364800	-1.31665400	-1.65882000
H	3.58214500	-1.26115500	-2.22975600
H	2.92607600	1.93466900	-1.65590300
H	1.05751900	3.09008800	-0.40761600
H	2.47970400	4.15103400	-0.60480200
H	2.14978500	3.37069300	0.96572300
H	4.71687700	3.35072800	-0.58447700
H	4.56510800	2.42944100	0.92689400
H	5.19068400	1.63952100	-0.55230000
H	0.84344900	2.75996900	-4.42181500
H	0.86117300	3.15725900	-2.68077900
H	1.34765700	1.52574000	-3.22063600
H	-1.46915600	2.74217600	-3.47420900

H	-0.60528900	-0.13122000	-4.16734000
H	-2.19521000	0.60651100	-4.48561700
H	-0.76500700	1.17515900	-5.38329100
H	1.64621606	-1.68145188	-4.00059949
H	1.77007208	-2.81996514	-2.78325104

**[SiP<sup>iPr</sup><sub>3</sub>]Fe=NNMe<sub>2</sub> (Charge = 0, S = 1/2)**

Fe	0.26930900	-0.39822500	-0.74095100
P	-0.81576500	-2.13248700	0.28435800
P	2.27538400	0.36262500	0.07732700
P	-1.23578900	1.19419600	-1.59406900
Si	-0.43496900	0.66804200	1.20952300
N	0.87532700	-1.07509800	-2.26051800
N	1.45742000	-1.90681400	-3.04479200
C	3.85243300	-0.67720900	-0.13235900
C	2.11104900	3.22224200	-0.12823300
C	3.74785900	-2.07344600	0.49721000
C	3.42392500	0.74149300	2.73562500
C	3.28944600	1.01336400	4.10780400
C	-1.78338800	-0.31804600	2.13235500
C	-3.19828500	-2.67782600	-1.26511700
C	2.98978500	2.03594000	-0.55540100
C	4.44928000	2.35966900	-0.16951000
C	-1.11083500	2.42518400	0.85890900
C	0.99316000	0.88501100	2.45933100
C	2.28228000	0.67655200	1.90721800
C	0.27930300	-3.41705700	1.20977400
C	-1.93511500	-3.33212400	-0.68902800
C	-1.96619500	-1.64305900	1.66180000
C	-1.36343100	2.69363800	-0.51361600
C	4.32331400	-0.75171100	-1.59703300
C	0.85020300	-2.79968700	2.49971100
C	0.87983500	1.16644400	3.83751100
C	0.64676600	2.35680800	-3.40893900
C	-3.11962500	0.91136300	-1.86842800
H	-3.15288100	-0.03454200	-2.44083300
C	-2.95493400	-2.46707800	2.24310900
C	2.01706300	1.23137100	4.66006700
C	-1.25254700	3.47556600	1.79001800
C	-3.85405300	0.70108200	-0.53367900
H	-3.91088800	1.64577800	0.03563900
H	-4.89000800	0.36023700	-0.72306700
H	-3.36153000	-0.04198500	0.10979500
C	-3.75897100	-1.98192100	3.28823700
C	-0.33628700	-4.79062300	1.54453600

C	-0.80732900	1.87015300	-3.31068900
C	-1.71713800	3.99457200	-0.92896600
C	-1.61105800	4.77021500	1.37544700
C	-2.59981700	0.15094500	3.18434800
C	-3.58112200	-0.67154300	3.76193600
C	-1.83079700	5.03170400	0.01339000
C	-1.18373400	-4.06783400	-1.80858500
C	-3.87344000	1.99143200	-2.67214700
H	-3.49103700	2.13808500	-3.69588800
H	-4.93751600	1.69752900	-2.76114500
H	-3.85040700	2.96450600	-2.15021900
C	-1.11632400	0.81858200	-4.39538900
H	-0.11197200	1.30411100	4.28645500
H	1.91086200	1.43534200	5.73235400
H	4.18079600	1.04627100	4.74544300
H	4.42614200	0.56314400	2.33021400
H	-1.04147100	3.29561400	2.85202700
H	-1.69760800	5.57934600	2.11069300
H	-2.08669700	6.04469900	-0.31928000
H	-1.88407900	4.21821200	-1.98901600
H	-2.49224600	1.18393500	3.53973000
H	-4.21616500	-0.28843200	4.56981200
H	-4.53124200	-2.62602400	3.72526700
H	-3.12362000	-3.48592600	1.87642700
H	-3.79224500	-2.15855600	-0.49627900
H	-2.93749100	-1.95125400	-2.05285300
H	-3.84178300	-3.45243900	-1.72608000
H	-2.25790400	-4.08274300	0.05642000
H	-0.84067100	-3.35185700	-2.57564800
H	-1.85737700	-4.79499700	-2.30204800
H	-0.30667800	-4.62638300	-1.43964900
H	1.28057800	-1.80011400	2.33317000
H	0.06187600	-2.69930100	3.26671100
H	1.64243000	-3.45216800	2.91410100
H	-1.20650200	-4.68875200	2.21773800
H	-0.64878500	-5.36525100	0.65652500
H	0.41377800	-5.40330800	2.08180800
H	1.12047000	-3.57984300	0.50789500
H	2.96890400	-2.67923000	0.00574800
H	3.50535900	-2.02026100	1.57152900
H	4.71069500	-2.61036900	0.39187300
H	4.62560800	-0.12435300	0.43293100
H	4.50048100	0.24402600	-2.03727200
H	5.27364800	-1.31665400	-1.65882000
H	3.58214500	-1.26115500	-2.22975600
H	2.92607600	1.93466900	-1.65590300

H	1.05751900	3.09008800	-0.40761600
H	2.47970400	4.15103400	-0.60480200
H	2.14978500	3.37069300	0.96572300
H	4.71687700	3.35072800	-0.58447700
H	4.56510800	2.42944100	0.92689400
H	5.19068400	1.63952100	-0.55230000
H	0.84344900	2.75996900	-4.42181500
H	0.86117300	3.15725900	-2.68077900
H	1.34765700	1.52574000	-3.22063600
H	-1.46915600	2.74217600	-3.47420900
H	-0.60528900	-0.13122000	-4.16734000
H	-2.19521000	0.60651100	-4.48561700
H	-0.76500700	1.17515900	-5.38329100
C	1.91965900	-3.25685800	-2.65811800
H	1.42721400	-4.02778900	-3.28057900
H	3.01484900	-3.34254400	-2.79776600
H	1.66606500	-3.41447600	-1.60294900
C	1.73613200	-1.57412100	-4.45581200
H	1.09627300	-2.17111500	-5.13580000
H	1.54068700	-0.50473800	-4.60666400
H	2.79503800	-1.79550600	-4.69189500

**[SiP<sup>iPr</sup><sub>3</sub>]<sub>3</sub>Fe-N<sub>2</sub> (Charge = 0, S = 1/2)**

Fe	0.03030300	0.00359200	-1.01067400
P	2.11256500	-0.93176800	-0.74397100
P	-0.04879100	2.24790600	-0.51838200
P	-2.04363600	-1.03166100	-0.74506500
Si	0.01999900	-0.16296800	1.26798800
C	1.77320800	-0.48518300	1.96451900
C	-1.11640300	-1.60366700	1.80938000
C	-2.01380000	-2.05917700	0.80341800
C	2.76447500	-0.76525300	0.98354700
C	-0.79827800	2.53426700	1.15650500
C	2.14989900	-2.83832300	-0.94553300
C	-0.66572900	1.43803300	2.05275800
N	0.06922500	0.29500800	-3.93333600
C	1.53143600	3.31948400	-0.31580200
C	2.17089300	-0.39141600	3.31543500
C	-2.81910600	-3.19486500	1.03689300
C	-3.82995000	0.64481500	0.73821300
C	4.11382400	-0.92683300	1.36394300
C	-1.07405300	-2.29465200	3.03932300
C	3.58505600	-0.48035800	-1.84378100
C	-1.13875700	1.58145200	3.37432000
C	1.33775100	-3.53778500	0.15779900

C	-1.02639300	3.39596800	-1.66646300
C	4.48703500	-0.81869900	2.71434100
C	2.37441300	2.85963800	0.88568000
C	3.55167400	-3.47872900	-1.01092800
C	3.51442400	-0.55702100	3.69272100
C	-2.45986100	-2.27637400	-2.10852700
C	-1.41636700	3.72705900	1.58850600
C	-3.74663000	-0.17734400	-0.55915600
C	-2.74955300	-3.87514600	2.26442300
C	1.32048800	4.84430200	-0.20940900
C	-0.30015900	3.63707200	-3.00737800
C	-1.88342600	-3.41941200	3.27134300
C	-1.74763200	2.77321700	3.80307700
C	-2.46009400	2.90795700	-1.92124700
C	-1.29736400	-3.24188600	-2.39067100
C	-2.91092100	-1.57540300	-3.40678500
C	-1.89545800	3.84246400	2.90497800
C	-4.97828400	-1.10253400	-0.64083500
C	3.34158200	-0.88580200	-3.31241700
C	3.97009200	1.00405900	-1.76213200
H	1.42766000	-0.15160300	4.08673300
H	3.80572100	-0.46547200	4.74586400
H	5.53942200	-0.93278400	2.99940800
H	4.88807400	-1.11972200	0.61268600
H	-1.55061300	4.56900700	0.90001500
H	-2.38874000	4.76760600	3.22558900
H	-2.12377900	2.86156400	4.82929700
H	-1.06492000	0.73894700	4.07420000
H	-0.37305800	-1.97240700	3.81989600
H	-1.82548000	-3.95167800	4.22831800
H	-3.36803800	-4.76512500	2.42939300
H	-3.49138900	-3.57404400	0.25920500
H	-5.05625200	-1.65920700	-1.58903000
H	-4.99190000	-1.82678600	0.19264000
H	-4.78318100	1.20671600	0.75954200
H	-3.00622900	1.36568200	0.83920500
H	-3.80947800	-0.01224400	1.62573400
H	-0.41364700	-2.69693300	-2.76668500
H	-1.00066600	-3.80621800	-1.49068900
H	-1.59547600	-3.97266400	-3.16669400
H	-3.21529400	-2.33707300	-4.14983800
H	-3.30944100	-2.87343700	-1.72521400
H	1.83016800	-3.43125000	1.14056400
H	0.31794300	-3.13750300	0.25359000
H	1.26272100	-4.61940800	-0.06407600
H	1.63914400	-3.00539600	-1.91310800

H	4.12490600	-3.28182700	-0.08708500
H	4.15253800	-3.14592300	-1.87293900
H	3.44085800	-4.57685000	-1.09507700
H	2.54291600	-0.27833500	-3.76786500
H	3.06229100	-1.94696700	-3.42838300
H	4.26497100	-0.71978000	-3.89950900
H	4.43616300	-1.07321300	-1.45707500
H	4.87984300	1.18834700	-2.36505300
H	3.16505800	1.63788500	-2.17187400
H	4.17665000	1.32868000	-0.72872900
H	1.87122900	3.10538900	1.83766100
H	2.56614000	1.77697300	0.88269100
H	3.35114500	3.38027500	0.87931500
H	2.09953400	3.10880800	-1.24114700
H	0.72545200	5.10398100	0.68437700
H	0.83568900	5.29097400	-1.09272000
H	2.30575200	5.33625100	-0.09481200
H	0.73656600	3.99221300	-2.88047900
H	-0.84453100	4.40660300	-3.58774200
H	-0.26913500	2.72159300	-3.61927000
H	-1.08863100	4.36399000	-1.13349600
H	-3.02831600	2.78540400	-0.98383200
H	-2.45638100	1.94277600	-2.45690000
H	-3.00058300	3.64026500	-2.55149700
H	-2.09353900	-0.98644300	-3.85322200
H	-3.77127100	-0.90156700	-3.25437500
H	-5.89316800	-0.48625500	-0.54826400
H	-3.77443000	0.51925200	-1.41696000
N	0.04804600	0.18304400	-2.80033200

**[SiP<sup>iPr</sup><sub>3</sub>]Fe-NH<sub>2</sub>NH<sub>2</sub> (Charge = 1, S = 1)**

Fe	0.05231400	0.06109300	-1.04623900
N	0.18879100	0.08871900	-3.15025700
N	-0.41736800	1.11083200	-3.98497200
P	0.74800000	2.29289500	-0.51844800
P	1.64293800	-1.70969800	-0.72429700
P	-2.26061000	-0.44993600	-0.61036800
Si	0.06165800	-0.06110300	1.25771300
C	1.14532900	1.29712700	2.03040100
C	1.45476200	2.39400800	1.18462200
C	2.25668700	3.45358700	1.66407000
C	2.75038700	3.42634200	2.97820500
C	2.44968000	2.34376400	3.82155900
C	1.65400300	1.28836100	3.34733200
C	0.66599100	-1.77493400	1.84227700

C	1.32733700	-2.57096600	0.86970700
C	1.73745900	-3.88587400	1.17830700
C	1.49677900	-4.41499000	2.45689900
C	0.85551600	-3.63309400	3.43166200
C	0.44238400	-2.32639600	3.12235500
C	-1.67626100	0.15814900	2.00002500
C	-2.76625000	-0.03166800	1.11217300
C	-4.09433100	0.05702800	1.59037600
C	-4.33786500	0.35803300	2.93972400
C	-3.26462000	0.57041000	3.82053900
C	-1.94577900	0.46799700	3.35077900
C	-0.56914400	3.65683800	-0.55065500
C	-1.72434700	3.35862600	0.42051300
C	-0.03972900	5.08037400	-0.27733500
C	2.10478000	3.07654400	-1.58842300
C	1.62022100	3.57758400	-2.96198500
C	3.32413400	2.15435200	-1.74221600
C	3.50927600	-1.32953400	-0.59323100
C	3.81869600	-0.54380100	0.69376700
C	4.43760400	-2.55938300	-0.67243200
C	1.67186400	-3.09517700	-2.01556400
C	2.26471600	-2.64654700	-3.36940200
C	0.31051100	-3.78034300	-2.21769300
C	-2.92090200	-2.21305700	-0.82202100
C	-2.26537100	-3.14398200	0.21560100
C	-4.45250200	-2.38954700	-0.75320300
C	-3.26925300	0.61004600	-1.83724000
C	-4.61425200	1.21485000	-1.38969100
C	-3.43172300	-0.12247400	-3.18947400
H	-0.09146100	-1.74246300	3.88223500
H	0.66266300	-4.04833800	4.42714300
H	1.80595000	-5.44017000	2.68800800
H	2.23138200	-4.51540400	0.42976100
H	-1.11558600	0.65492800	4.04297300
H	-3.45717200	0.81989800	4.86999900
H	-5.36968600	0.43459400	3.29960100
H	1.45382100	0.43227300	4.00366200
H	2.84642900	2.31756800	4.84263600
H	3.37871900	4.24788100	3.33911100
H	2.51566600	4.30186600	1.02178400
H	-2.19603400	2.38183500	0.23666300
H	-1.37556500	3.36198300	1.46827700
H	0.77208500	5.39312400	-0.95381600
H	0.31751800	5.17294100	0.76285200
H	2.43068600	3.95646600	-1.00227300
H	3.07770500	1.25870900	-2.34340400

H	3.72110100	1.81811900	-0.77071500
H	0.83756200	4.35035100	-2.88309700
H	1.21171300	2.76360300	-3.58424200
H	2.47264100	4.03038400	-3.50191200
H	1.20303500	0.16074900	-3.31665100
H	-0.08270800	-0.85858300	-3.46291200
H	-0.53716900	0.75068100	-4.94276000
H	-1.35302900	1.29358400	-3.60914500
H	4.87086400	-0.20510500	0.67497000
H	3.68764400	-1.18092200	1.58560100
H	4.22639300	-3.27435800	0.14204000
H	5.48298900	-2.22301700	-0.54383800
H	4.38630200	-3.09590200	-1.63379300
H	3.71682200	-0.67367800	-1.46042300
H	2.36237500	-3.84734800	-1.59171500
H	3.19221400	-2.05769500	-3.27003300
H	2.50275500	-3.53468300	-3.98259500
H	1.54560500	-2.05057600	-3.96118600
H	-0.05737300	-4.25260800	-1.29308600
H	-0.46327200	-3.06707000	-2.56069600
H	0.39672800	-4.56946800	-2.98762000
H	-2.61623400	-2.90223800	1.23390700
H	-1.16751900	-3.07301800	0.21917100
H	-2.57728100	-2.50655800	-1.83334700
H	-2.54701900	-4.19193200	0.00381100
H	-4.70261500	-3.43696500	-1.00533500
H	-4.82490900	-2.20669000	0.26882900
H	-5.01228700	-1.74248600	-1.44677900
H	-2.51432900	-0.64539600	-3.51523700
H	-4.23302100	-0.87765000	-3.14403400
H	-3.71371400	0.59677800	-3.98101500
H	-4.94592800	-0.09277200	0.92257800
H	-5.38981000	0.44446400	-1.24095400
H	-4.98133400	1.89804900	-2.17869900
H	-4.52133900	1.79772900	-0.45988900
H	-2.58173700	1.46885100	-1.98682200
H	-0.95447200	3.61344500	-1.58944000
H	-2.50057400	4.13993400	0.32385800
H	-0.86808900	5.80165000	-0.40386900
H	4.13373300	2.68863800	-2.27258800
H	3.17516800	0.33977300	0.82000600

## Electrochemistry

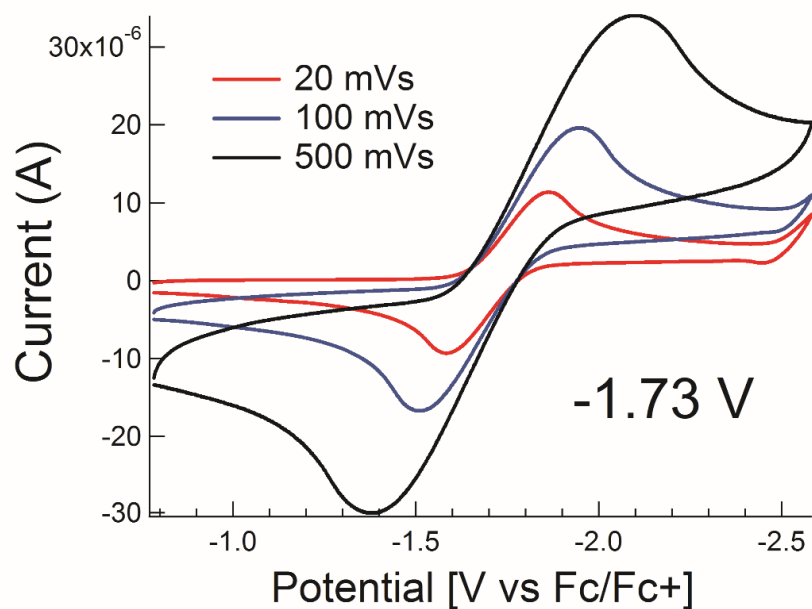


**Figure S44.** Cyclic voltammograms obtained on THF solutions of 1 mM **6** (298 K, 0.1 M tetra-*n*-butylammonium hexafluorophosphate) at the listed scan rate.

## Variable Temperature NMR Data on Compound 6

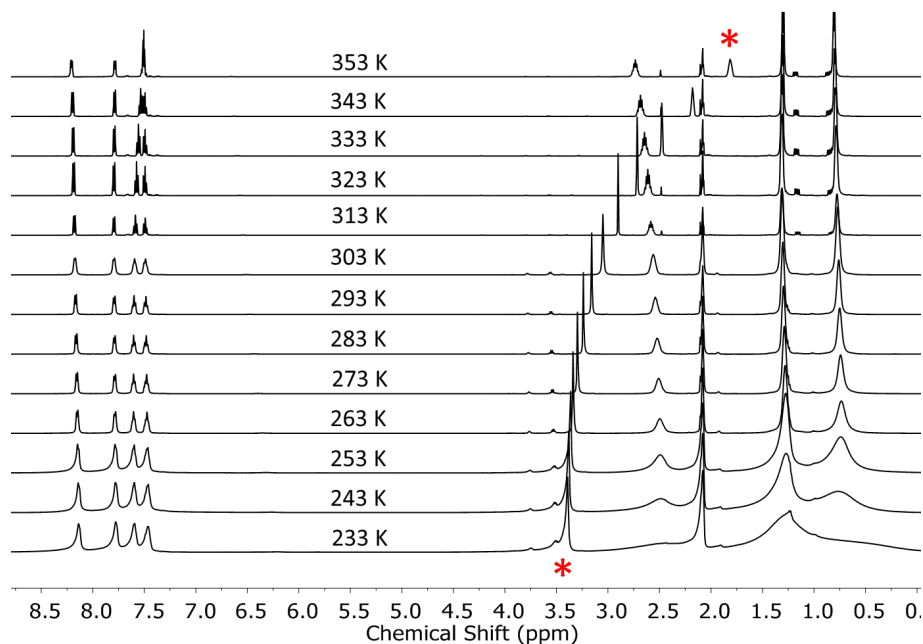


**Figure S45.**  $^1\text{H}$  NMR spectra (500 MHz, listed temperatures) of **6** recorded in  $\text{CD}_3\text{CN}$ . The asterisk denotes the resonance assigned to the  $\text{NN}(\text{CH}_3)_2$  protons.

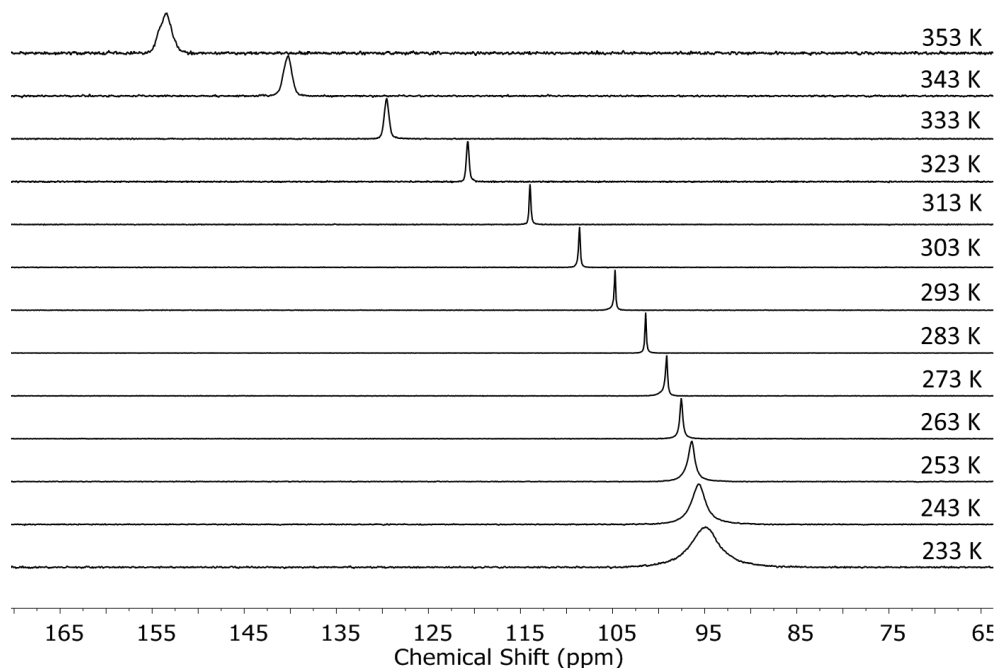


**Figure S46.**  $^{31}\text{P}$  NMR spectra (202.4 MHz, listed temperatures) of **6** recorded in  $\text{CD}_3\text{CN}$ .

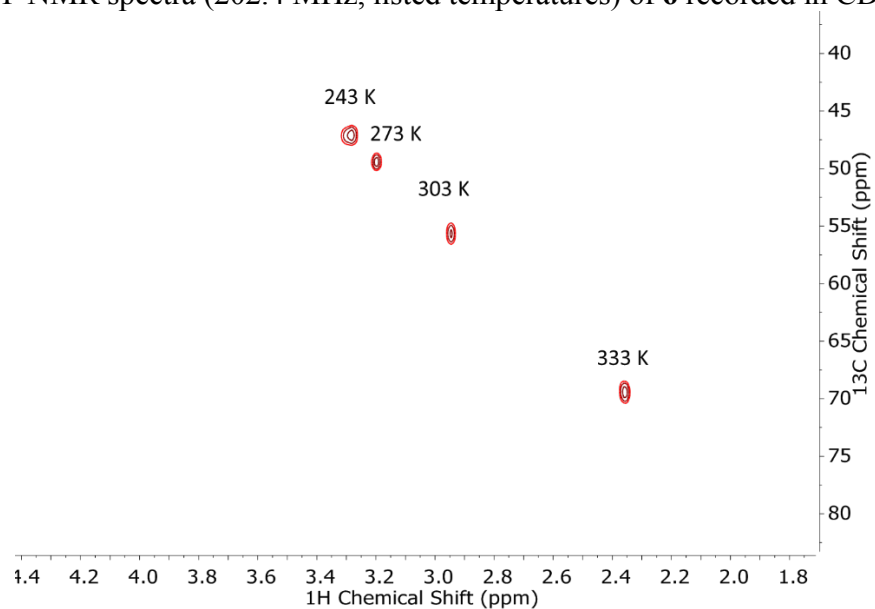


**Figure S47.** Stacked  $^1\text{H}$ - $^{13}\text{C}$  HMQC NMR spectra (125.7 MHz, listed temperatures) of **6** recorded in  $\text{CD}_3\text{CN}$ .

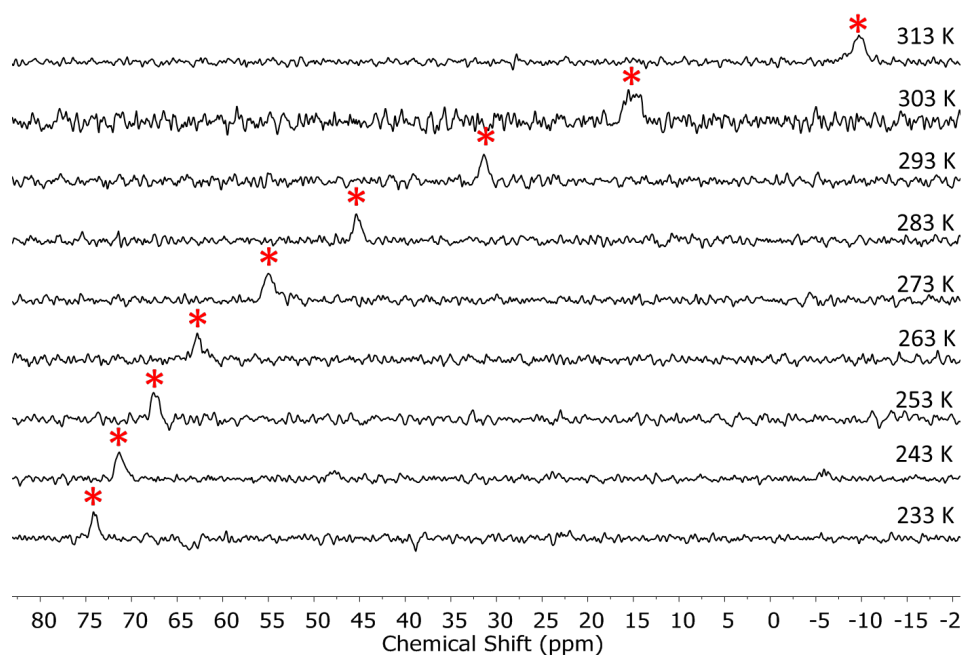


**Figure S48.**  $^{29}\text{Si}$  NMR spectra (99.3 MHz, listed temperatures) of **6** recorded in  $\text{CD}_3\text{CN}$ .

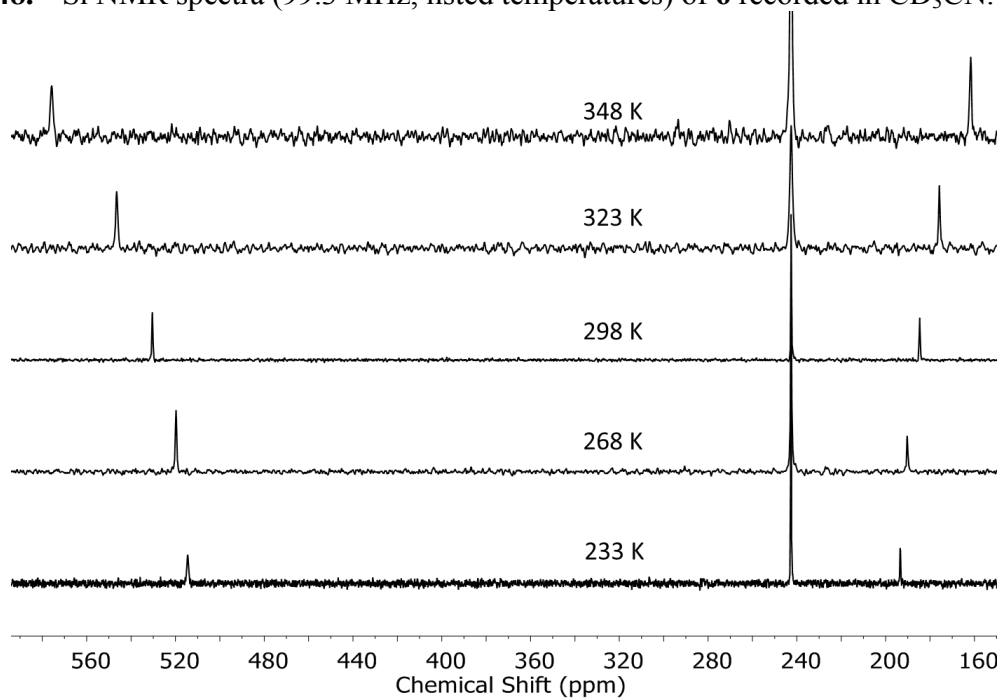


**Figure S49.**  $^{15}\text{N}$  NMR spectra (50.6 MHz, listed temperatures) of  $^{15}\text{N}$ -**6** recorded in  $\text{CD}_3\text{CN}$  ( $\text{CD}_3^{15}\text{C}$  located at 242.6 ppm).

At elevated temperatures, compound **6** displays temperature-dependent paramagnetism, consistent with the thermal population of an excited triplet state. On warming  $\text{CD}_3\text{CN}$  solutions of **6**, the chemical shifts of resonances in the  $^1\text{H}$ ,  $^{13}\text{C}$ ,  $^{15}\text{N}$ ,  $^{31}\text{P}$ , and  $^{29}\text{Si}$  NMR spectra dramatically move in a non-linear and non-exponential fashion (Figures S45-49). The variable temperature behavior of the  $^{31}\text{P}$ ,  $^{29}\text{Si}$ , and  $[\text{NN}(\text{CH}_3)_2]\text{-}^1\text{H}$  resonances can be simulated by an excited-state

magnetization function (Eqn S3), indicating that **6** possesses a low-lying triplet state 6.7(3) kcal/mol above the ground singlet state.

$$f(T) = A + (B * \text{EXP}(C / (8.3145 * T))) / ((1 + 3 * \text{EXP}(C / (8.3145 * T))) * T) \quad \text{Eqn S3}$$

Where **A**, **B** and **C** are fit constants and T is the temperature in Kelvin. **A** is the chemical shift (in ppm) of the diamagnetic ground state at 0 K, **B** is proportional to the hyperfine coupling constant, and **C** is the difference in energy between the ground and excited states in Joules.

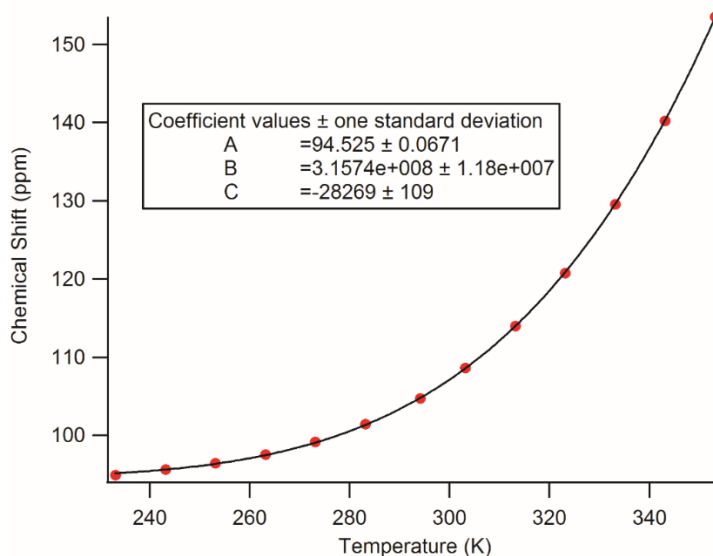


**Figure S50.** The temperature dependence of the  $^{31}\text{P}\{^1\text{H}\}$  NMR chemical shift of **6** fit to equation S3. The resulting best fit parameters are listed in the legend.

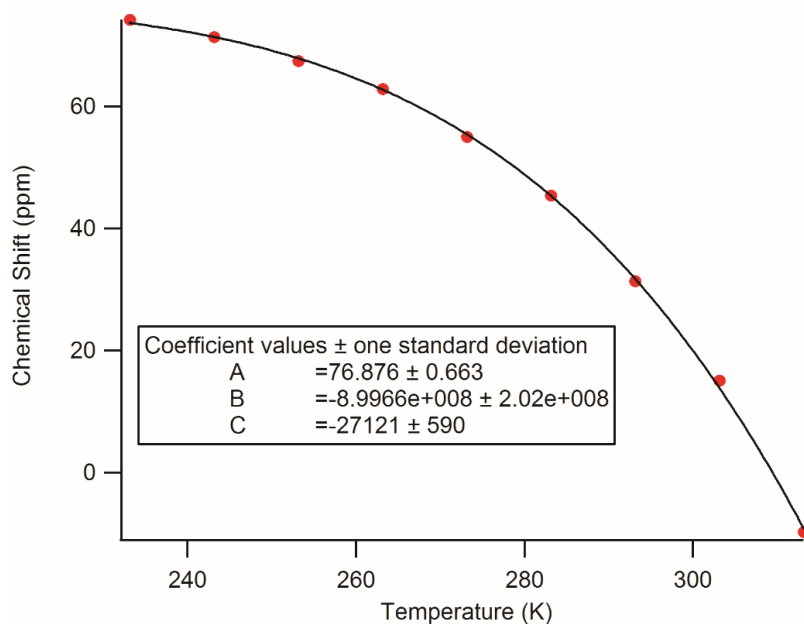


**Figure S51.** The temperature dependence of the  $^{29}\text{Si}\{^1\text{H}\}$  NMR chemical shift of **6** fit to equation S3. The resulting best fit parameters are listed in the legend.

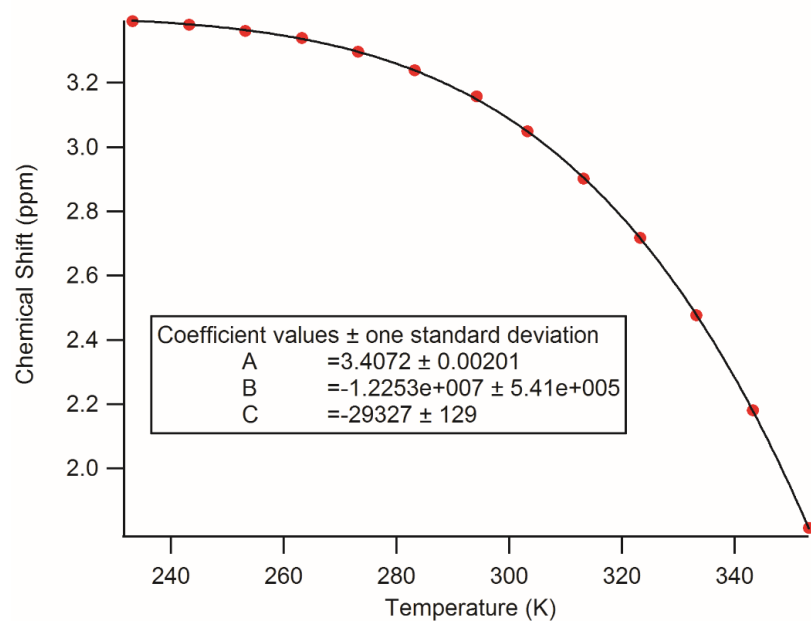


**Figure S52.** The temperature dependence of the  $^1\text{H}$  NMR chemical shift of the  $\text{FeNN}(\text{CH}_3)_2$  protons in **6** fit to equation S3. The resulting best fit parameters are listed in the legend.

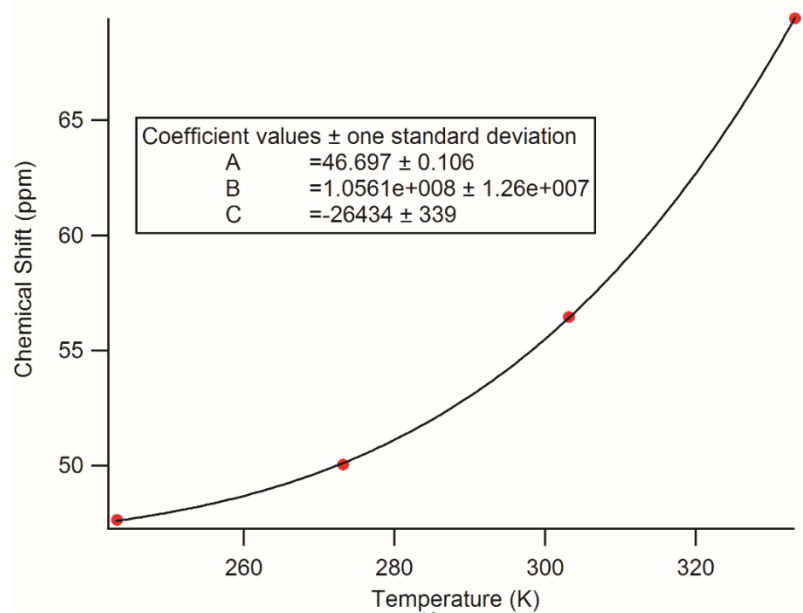


**Figure S53.** The temperature dependence of the  $^{13}\text{C}$  NMR chemical shift of the  $\text{FeNN}(\text{CH}_3)_2$  carbons in **6** fit to equation S3. The resulting best fit parameters are listed in the legend.

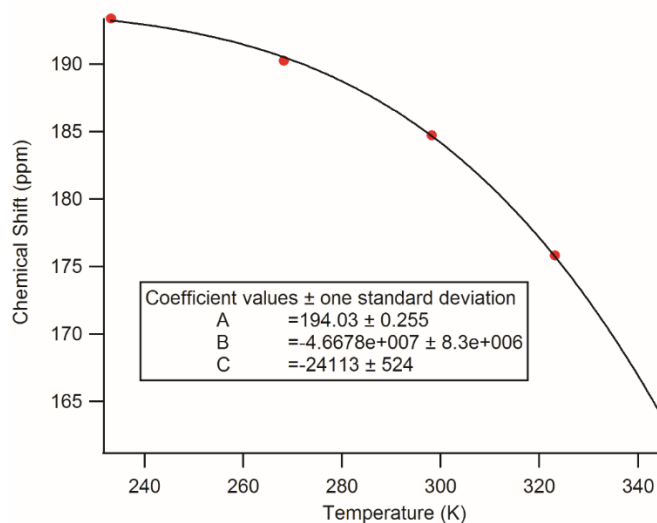


**Figure S54.** The temperature dependence of the  $^{15}\text{N}$  NMR chemical shift of the beta nitrogen of **6** fit to equation S3. The resulting best fit parameters are listed in the legend.

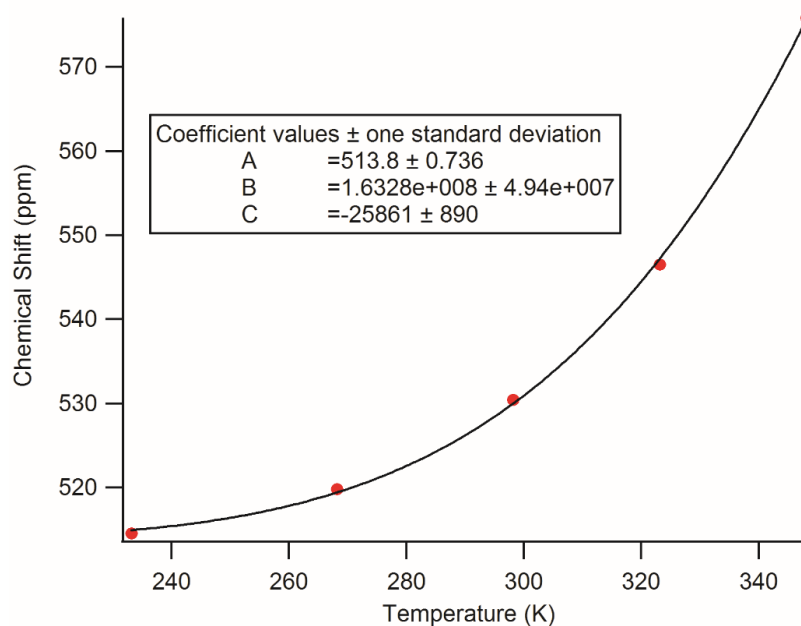


**Figure S55.** The temperature dependence of the  $^{15}\text{N}$  NMR chemical shift of the alpha nitrogen of **6** fit to equation S3. The resulting best fit parameters are listed in the legend.

#### Cited References.

1. Lee, Y.; Mankad, N. P.; Peters, J. C. *Nat. Chem.* **2010**, *2*, 558-565.
2. Brookhart, M.; Grant, B.; Volpe, A. F. *Organometallics* **1992**, *11*, 3920.
3. Berto, T. C.; Hoffman, M. B.; Murata, Y.; Landenberger, K. B.; Alp, E. E.; Zhao, J. Y.; Lehnert, N. *J. Am. Chem. Soc.* **2011**, *133*, 16714.
4. Evans, D. F. *J. Chem. Soc.* **1959**, 2003.
5. Stoll, S.; Schweiger, A. *J. Magn. Reson.* **2006**, *178*, 42.
6. Münck, E. *Aspects of  $^{57}\text{Fe}$  Mössbauer Spectroscopy*; University Science Books: Sausalito, CA, 2000.

7. Gaussian 09, Revision B.01, Frisch, M. J.; Trucks, G. W.; Schlegel, H. B.; Scuseria, G. E.; Robb, M. A.; Cheeseman, J. R.; Scalmani, G.; Barone, V.; Mennucci, B.; Petersson, G. A.; Nakatsuji, H.; Caricato, M.; Li, X.; Hratchian, H. P.; Izmaylov, A. F.; Bloino, J.; Zheng, G.; Sonnenberg, J. L.; Hada, M.; Ehara, M.; Toyota, K.; Fukuda, R.; Hasegawa, J.; Ishida, M.; Nakajima, T.; Honda, Y.; Kitao, O.; Nakai, H.; Vreven, T.; Montgomery, J. A., Jr.; Peralta, J. E.; Ogliaro, F.; Bearpark, M.; Heyd, J. J.; Brothers, E.; Kudin, K. N.; Staroverov, V. N.; Kobayashi, R.; Normand, J.; Raghavachari, K.; Rendell, A.; Burant, J. C.; Iyengar, S. S.; Tomasi, J.; Cossi, M.; Rega, N.; Millam, J. M.; Klene, M.; Knox, J. E.; Cross, J. B.; Bakken, V.; Adamo, C.; Jaramillo, J.; Gomperts, R.; Stratmann, R. E.; Yazyev, O.; Austin, A. J.; Cammi, R.; Pomelli, C.; Ochterski, J. W.; Martin, R. L.; Morokuma, K.; Zakrzewski, V. G.; Voth, G. A.; Salvador, P.; Dannenberg, J. J.; Dapprich, S.; Daniels, A. D.; Farkas, Ö.; Foresman, J. B.; Ortiz, J. V.; Cioslowski, J.; Fox, D. J. Gaussian, Inc., Wallingford CT, 2009.
8. Watt, G. W.; Chrisp, J. D. *Anal. Chem.* **1952**, 24, 2006-2008.
9. Weatherburn, M. W. *Anal. Chem.* **1967**, 39, 971-974.
10. Pfirrmann, S.; Limberg, C.; Herwig, C.; Knispel, C.; Braun, B.; *et al.* *J. Am. Chem. Soc.* **2010**, 132, 13684-13691